Exploring and Expanding the Three-Dimensional Structural Diversity of Supramolecular Dendrimers with the Aid of Libraries of Alkali Metals of Their AB_3 Minidendritic Carboxylates

Virgil Percec,*[a] Marian N. Holerca,[a] Satoshi Uchida,[a] Wook-Dong Cho,[a] Goran Ungar,[b] Yongsong Lee,[b] and Duncan J. P. Yeardley[b]

Abstract: The synthesis of the alkali metal salts of 3,4,5-tris(*n*-alkan-1-yloxy)-benzoic acid [**(3,4,5)*n*G1-CO_2M**, where *n* is the number of methylenic units in the alkane group for $n = 12$, 14, 16, 18 and M = Li, Na, K, Rb, Cs] is described. The structural analysis of these AB_3 molecules by a combination of methods which includes X-ray diffraction experiments was performed. These experiments have demonstrated that **(3,4,5)*n*G1-CO_2M** self-assemble at low temperatures into supramolecular cylinders and at high temperatures into spheres which subsequently self-organize into two-dimensional *c2mm* rectangular columnar, *p6mm* hexagonal columnar, three-dimensional $Pm\bar{3}n$ and $Im\bar{3}m$ cubic lattices. In addition a novel unidentified liquid crystalline lattice was also discovered. The dependence between the symmetry of the lattice and the molecular structure of **(3,4,5)*n*G1-CO_2M** was established. **(3,4,5)*n*G1-CO_2M** represents one of the AB_3 minidendrons (i.e., first-generation monodendron attached to the periphery of larger generation dendrons) that is responsible for the control of the three-dimensional structures created from libraries of larger generations of dendrimers. Therefore, the molecular structure–lattice dependence elaborated here will aid the rational design of the three-dimensional shapes from larger generations of supramolecular dendrimers and of their lattices. In addition, the temperature responsive shape change of these supramolecular objects may generate new supramolecular concepts and technological applications.

Keywords: alkali metals · dendrimers · lattices · self-assembly · supramolecular chemistry

Introduction

In a series of previous publications from our laboratory we have reported the design and the structural analysis of the first libraries of AB_3 and AB_2 monodendrons which self-assemble into soft-objects that self-organize in three-dimensional $Pm\bar{3}n$[1] and $Im\bar{3}m$[2] cubic and two-dimensional *p6mm*[3] hexagonal columnar lattices (Scheme 1). This concept is currently under investigation also in other laboratories.[4] These self-assembling monodendrons provide building blocks for the construction of complex macromolecular and supramolecular systems[5] and for the elaboration of new concepts at the interface between organic, macromolecular, and supramolecular chemistry.[6] In a recent publication[1g] we have demonstrated that for the same generation number the shape and size of the self-assembling monodendron and of the corresponding supramolecular dendrimer is determined by the architecture of the first-generation monodendron attach-

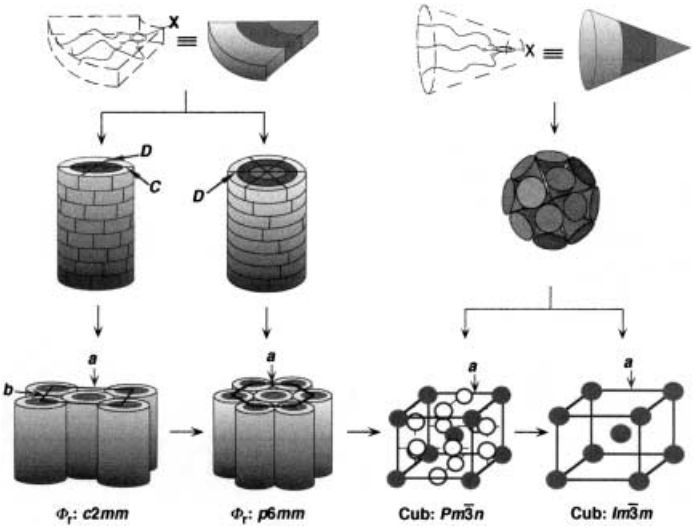

Scheme 1. Schematic representation of the generation of synthetic supramolecular architectures via self-assembly and self-organization of flat-taper and conical dendritic building blocks.

[a] Prof. V. Percec, Dr. M. N. Holerca, Dr. S. Uchida, W.-D. Cho
Roy & Diana Vagelos Laboratories
Department of Chemistry, University of Pennsylvania
Philadelphia, PA 19104-6323 (USA)
Fax: (+1) 215-573-7888
E-mail: percec@sas.upenn.edu

[b] Dr. G. Ungar, Y. Lee, D. J. P. Yeardley
Department of Engineering Materials and Center
for Molecular Materials, University of Sheffield
Sheffield S1 3JD (UK)

0947-6539/02/0805-1106 $ 17.50+.50/0

ed to their periphery. Several years ago we have coined the name minimonodendron[7] for the first generation of a self-assembling monodendron. The role of these minimonodendrons is analogous to that of simple peptides used in the understanding of the molecular engineering involved in the assembly of more complex proteins, or of maquettes used by sculptors and architects to appreciate various aspects of full-size objects.[8] To date we have demonstrated that self-assembling minimonodendrons are extremely useful as maquettes for larger generations of monodendrons. This is the case especially when the functionality attached to their focal point enables to simulate some of the functions of the inner part of the larger generations of dendrons. In this particular case a detailed analysis of the three-dimensional structures of the larger supramolecular dendrimers as well as the discovery of new structures and structural concepts[7, 9] accessible through larger molecules can be obtained from the investigation of minimonodendrons. The minidendritic approach to the discovery and elucidation of novel supramolecular structures, lattices, and structural concepts that are subsequently encountered in larger generations of supramolecular dendrimers is less time demanding and much less expensive than the conventional direct process.

The library of monodendrons investigated in our laboratory contains an aromatic AB_3 or AB_2 poly(benzyl ether) inner part[1g] and an outer part containing an AB_3 or AB_2 benzyl ether substituted with hydrogenated,[1g] or fluorinated[1b] alkyl groups. By increasing the generation number of the monodendron the interaction between the larger number of benzyl ether inner units increases to the point that it can compete and dominate the interactions generated from the functional group attached to their focal point.

The simplest library of minimonodendrons that is expected to simulate the trend exploited by larger generations of AB_3 dendrons without requiring the effort involved in their synthesis consists of the much less demanding synthesis of alkali metal salts of 3,4,5-tris(*n*-alkan-1-yloxy)benzoic acid [**(3,4,5)*n*G1-CO$_2$M**, where *n* is the number of methylene units in the alkane group and M is the alkali metal]. Metal salts and other metal complexes have been previously used[10–12] to generate various organized assemblies. The corresponding 3,4,5-tris(*n*-dodecan-1-yloxy)benzyl ether unit has been employed as one of the minidendritic units attached to the periphery of larger self-assembling dendrons.[1g] The size of the alkali metal present in the focal point of **(3,4,5)*n*G1-CO$_2$M** affects both the strength of the interaction in the core of the supramolecular minidendrimer and the solid angle of the minimonodendron.[9] These two parameters have dominant contributions to the determination of the shape and size of the larger generations of supramolecular dendrimers.[1g]

This publication reports the synthesis and the structural analysis of **(3,4,5)*n*G1-CO$_2$M** with $n = 12$, 14, 16, 18 and M = Li, Na, K, Rb, Cs. These experiments will demonstrate the capability of the minidendritic concept to contribute to the discovery of new two- and three-dimensional shapes and lattices from larger generations of supramolecular dendrimers and to the elucidation of the dependence between the molecular structure and the three-dimensional structures of supramolecular dendrimers.

Results and Discussion

Synthesis of (3,4,5)*n*G1-CO$_2$M: The synthesis of **(3,4,5)*n*G1-CO$_2$M** with M = Li, Na, K, Rb and Cs and $n = 12$, 14, 16 and 18 is outlined in Scheme 2. The synthesis of **(3,4,5)12G1-CO$_2$Na**, **(3,4,5)12G1-CO$_2$Cs**, **(3,4,5)14G1-CO$_2$Cs**, and **(3,4,5)16G1-CO$_2$Cs** was reported previously;[9b] the procedure used for the preparation of the other **(3,4,5)*n*G1-CO$_2$M** derivatives is an improvement of the previous methods.[13] In the first step methyl gallate was etherified with the corresponding 1-bromoalkane in DMF at 70 °C in the presence of K_2CO_3 as base. The alkali metal salts were prepared by the base-assisted hydrolysis of the methyl benzoates **(3,4,5)*n*G1-CO$_2$CH$_3$** with the corresponding alkali metal hydroxides (MOH) in EtOH (90 %) at 95 °C. The reaction was carried out under reflux for 10 h. After cooling to room temperature the resulting precipitate was filtered off and recrystallized from EtOH (90 %), dried under vacuum at 23 °C and freeze-dried from benzene. The yields of **(3,4,5)*n*G1-CO$_2$M** were in the range of 69.3 to 73.4 %. Certain salts contain water of hydration. The content of H_2O in each salt was determined by elemental analysis (Table 1) and is strongly dependent on the nature of alkali metal M in the salt and the number of carbons in the alkyl tail. Regardless of the number of carbons in the alkyl tails Li salts are free of water of solvation. In the case of 12 methylene units in the salts based on larger cations are solvated. Only the Na and K salts containing 14 and 16 carbons in the alkyl tail are solvated. All salts containing 18 carbons in the tail are unsolvated.

Structural and retrostructural analysis of the lattices generated from (3,4,5)*n*G1-CO$_2$M: The structure of the supramolecular dendrimers was determined by a combination of differential scanning calorimetry (DSC), thermal optical polarized microscopy (TOPM), and X-ray diffraction (XRD) experiments according to methods elaborated previously in our laboratory.[1–3] Second heating DSC scans of the **(3,4,5)*n*G1-CO$_2$M** are shown in Figure 1. The nature of the lattices observed for these compounds was determined by synchrotron radiation XRD experiments and is depicted in Figure 1. The structure of each lattice is shown in Scheme 1. As we can observe from Figure 1 each compound shows a

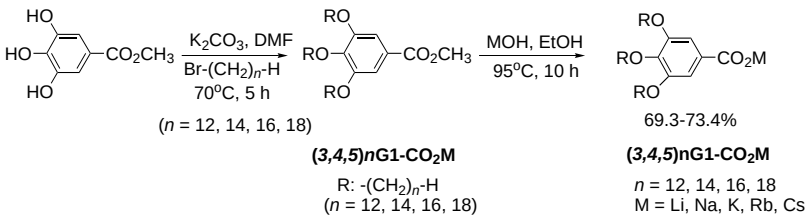

Scheme 2. The synthesis of minidendritic carboxylate salts **(3,4,5)*n*G1-CO$_2$M**.

Table 1. Calculated and experimental elemental analysis data of minimonodendrons **(3,4,5)*n*G1-CO$_2$M**.

Minimonodendron	Formula	Calculated	Experimental
(3,4,5)12G1-CO$_2$Li	$C_{43}H_{77}LiO_5$	C 75.84	C 75.56
		H 11.40	H 11.38
(3,4,5)12G1-CO$_2$Na	$C_{43}H_{77}NaO_5 \times 0.5\,H_2O$	C 73.15	C 73.18
		H 11.13	H 11.13
(3,4,5)12G1-CO$_2$K	$C_{43}H_{77}KO_5 \times 0.5\,H_2O$	C 71.51	C 71.94
		H 10.89	H 10.90
(3,4,5)12G1-CO$_2$Rb	$C_{43}H_{77}O_5Rb \times 0.5\,H_2O$	C 67.20	C 67.29
		H 10.23	H 10.22
(3,4,5)12G1-CO$_2$Cs	$C_{43}H_{77}CsO_5 \times 0.5\,H_2O$	C 63.29	C 63.84
		H 9.63	H 9.62
(3,4,5)14G1-CO$_2$Li	$C_{49}H_{89}LiO_5$	C 76.91	C 76.80
		H 11.72	H 11.70
(3,4,5)14G1-CO$_2$Na	$C_{49}H_{89}NaO_5 \times 0.5\,H_2O$	C 74.48	C 74.21
		H 11.48	H 11.49
(3,4,5)14G1-CO$_2$K	$C_{49}H_{89}KO_5 \times 0.5\,H_2O$	C 72.99	C 72.52
		H 11.25	H 11.27
(3,4,5)14G1-CO$_2$Rb	$C_{49}H_{89}O_5Rb$	C 69.76	C 69.53
		H 10.63	H 10.64
(3,4,5)14G1-CO$_2$Cs	$C_{49}H_{89}CsO_5$	C 66.04	C 66.10
		H 10.07	H 10.12
(3,4,5)16G1-CO$_2$Li	$C_{55}H_{101}LiO_5$	C 77.78	C 77.62
		H 11.99	H 11.92
(3,4,5)16G1-CO$_2$Na	$C_{55}H_{101}NaO_5 \times 0.5\,H_2O$	C 75.55	C 75.44
		H 11.76	H 11.76
(3,4,5)16G1-CO$_2$K	$C_{55}H_{101}KO_5 \times 0.5\,H_2O$	C 74.18	C 73.84
		H 11.55	H 11.55
(3,4,5)16G1-CO$_2$Rb	$C_{55}H_{101}O_5Rb$	C 71.20	C 71.08
		H 10.97	H 10.92
(3,4,5)16G1-CO$_2$Cs	$C_{55}H_{101}CsO_5$	C 67.73	C 67.62
		H 10.44	H 10.41
(3,4,5)18G1-CO$_2$Li	$C_{61}H_{113}LiO_5$	C 78.49	C 78.40
		H 12.20	H 12.19
(3,4,5)18G1-CO$_2$Na	$C_{61}H_{113}NaO_5$	C 77.16	C 77.19
		H 12.00	H 11.93
(3,4,5)18G1-CO$_2$K	$C_{61}H_{113}KO_5$	C 75.87	C 75.55
		H 11.79	H 11.68
(3,4,5)18G1-CO$_2$Rb	$C_{61}H_{113}O_5Rb$	C 72.40	C 70.04
		H 11.25	H 11.36
(3,4,5)18G1-CO$_2$Cs	$C_{61}H_{113}CsO_5$	C 69.15	C 69.11
		H 10.75	H 10.73

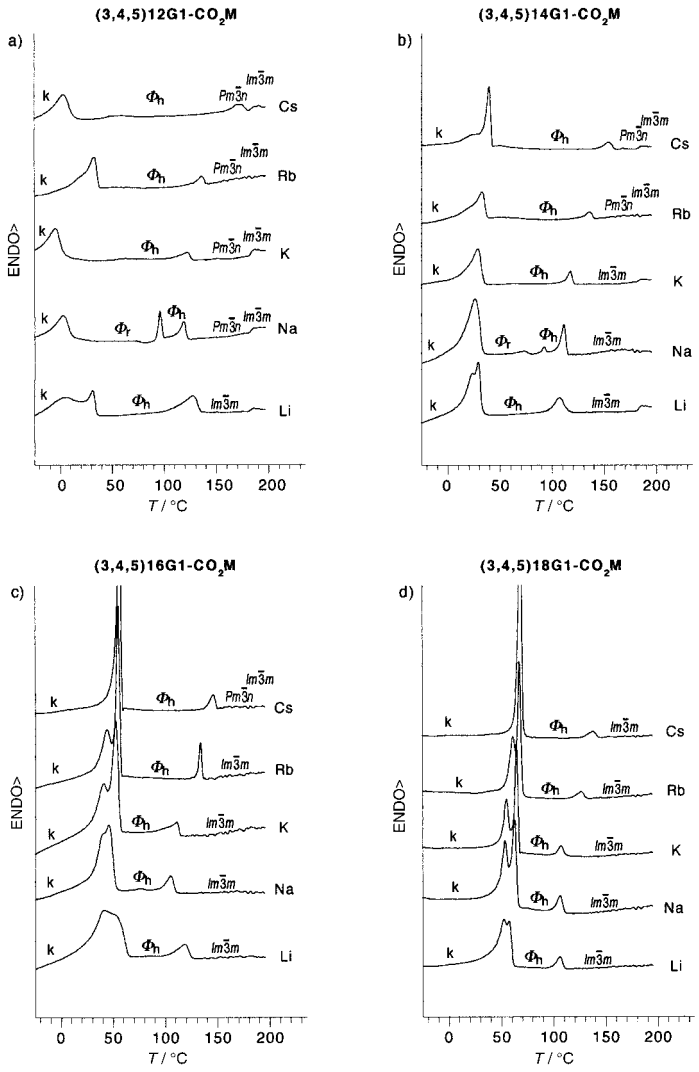

Figure 1. DSC traces (second heating scans) of **(3,4,5)*n*G1-CO$_2$M** and corresponding phase transition assigned according to XRD and TOPM: a) $n = 12$; b) $n = 14$; c) $n = 16$; d) $n = 18$ (with M = Li, Na, K, Rb and Cs).

complex phase behavior that is determined by the nature of alkali metal M and for the same M by the number of CH_2 in the alkyl tail and by temperature. None of these compounds exhibits a disordered liquid state (isotropic state) before their decomposition temperature. In addition, some of the cubic phases are not separated by a first order phase transition that can be observed on their DSC scans and therefore, since they are optically isotropic, their phase behavior could be determined only by XRD experiments.

Let us discuss briefly the dependence between the molecular structure of **(3,4,5)*n*G1-CO$_2$M** and their supramolecular structure starting with **(3,4,5)12G1-CO$_2$M** (Figure 1a). All salts exhibit a crystalline phase at low temperatures. This crystal phase was not analyzed by XRD (Figure 1). **(3,4,5)12G1-CO$_2$Li** displays a *p6mm* hexagonal columnar[3] (Φ_h) followed by an $Im\bar{3}m$ cubic lattice.[2] **(3,4,5)12G1-CO$_2$Na** exhibits *c2mm* rectangular columnar (Φ_r) followed by $Pm\bar{3}n$[1a] and $Im\bar{3}m$[2] cubic lattices. **(3,4,5)12G1-CO$_2$K**, **(3,4,5)12G1-CO$_2$Rb**, and **(3,4,5)12G1-CO$_2$Cs** show Φ_h followed by $Pm\bar{3}n$ and $Im\bar{3}m$ lattices. The rectangular columnar two-dimensional lattice (Φ_r) detected in **(3,4,5)12G1-CO$_2$Na** was not observed previously in supramolecular dendrimers.[1g, 4] Only a rectangular columnar of *p2gg* symmetry was previously observed in supramolecular dendrimers.[4b] However, c*2mm* rectangular columnar lattice was previously encountered in a series of tetrapalladium complexes.[10e]

Increasing the number of carbons in the alkyl tail from 12 to 14 produces **(3,4,5)14G1-CO$_2$M** (Figure 1b) which exhibits a slightly different behavior than **(3,4,5)12G1-CO$_2$M**. The Li salt **(3,4,5)14G1-CO$_2$Li** shows the same sequence of phases as **(3,4,5)12G1-CO$_2$Li**, that is, hexagonal columnar (Φ_h) followed by $Im\bar{3}m$ cubic. However, while **(3,4,5)12G1-CO$_2$Na** undergoes the sequence Φ_r, Φ_h, $Pm\bar{3}n$, $Im\bar{3}m$, **(3,4,5)14G1-CO$_2$Na** has the sequence Φ_r, Φ_h, $Im\bar{3}m$. Therefore, **(3,4,5)14G1-CO$_2$Na** changes its structure from Φ_h directly into $Im\bar{3}m$ without passing through the intermediary $Pm\bar{3}n$ cubic lattice. **(3,4,5)14G1-CO$_2$K** does not exhibit the $Pm\bar{3}n$ phase which is available in **(3,4,5)12G1-CO$_2$K** and therefore, **(3,4,5)14G1-CO$_2$K** displays the sequence Φ_h, $Im\bar{3}m$. **(3,4,5)14G1-CO$_2$M** with M = Rb and Cs shows an identical sequence of phases as the corresponding **(3,4,5)12G1-CO$_2$M**, that is, Φ_h, $Pm\bar{3}n$, $Im\bar{3}m$.

0947-6539/02/0805-1108 $ 17.50+.50/0 *Chem. Eur. J.* **2002**, *8*, No. 5

The increase in the number of carbons in the alkyl tail from 14 to 16 simplifies the phase behavior even more (Figure 1c). With the exception of **(3,4,5)16G1-CO_2Cs** which displays the sequence Φ_h, $Pm\bar{3}n$, $Im\bar{3}m$, all other salts exhibit a Φ_h followed by an $Im\bar{3}m$ phase. All **(3,4,5)18G1-CO_2M** display a Φ_h followed by an $Im\bar{3}m$ phase (Figure 1d). The other quantitative trend observed by inspecting Figure 1 is an increase of the phase transition temperature by increasing the size of the alkali metal of **(3,4,5)14G1-CO_2M**.

Figure 2 presents four representative examples of XRD experiments recorded as a function of temperature on the synchrotron. These XRD experiments were performed for all samples in order to provide information on the lattices discussed in Figure 1. **(3,4,5)16G1-CO_2Li** (Figure 2a) is an example that exhibits the sequence Φ_h (*p6mm*), $Im\bar{3}m$. **(3,4,5)14G1-CO_2Na** (Figure 2b) shows the sequence Φ_r (*c2mm*), Φ_h (*p6mm*), $Im\bar{3}m$, while **(3,4,5)14G1-CO_2Rb** (Figure 2c) demonstrates the sequence Φ_h (*p6mm*), $Pm\bar{3}n$, $Im\bar{3}m$. Finally, **(3,4,5)18G1-CO_2Rb** shows the sequence of phases Φ_h (*p6mm*), unknown new liquid crystal (LC), $Im\bar{3}m$. This new unknown LC phase was discussed in several other compounds and the elucidation of its lattice and supramolecular structure is in progress.

The summary of the transition temperatures and corresponding thermodynamic parameters collected from the DSC traces from Figure 1 and from the first heating and cooling DSC scans (not shown in Figure 1) is presented in Tables 2–5.

The retrostructural analysis by XRD experiments of the lattices exhibited by all these compounds according to procedures described in previous publications[1g] was performed. Table 6 summarizes *d*-spacings obtained from the X-ray experiments. Table 7 summarizes the XRD results for the cylindrical supramolecules which self-organize in *c2mm* rectangular and *p6mm* hexagonal columnar lattices. Table 8 summarizes the results for the spherical supramolecules that self-organize in $Pm\bar{3}n$ and $Im\bar{3}m$ lattices.

The transition temperatures from Tables 2–5 are plotted as a function of cation diameter in Figure 3. The corresponding enthalpy changes are plotted as a function of cation diameter in Figure 4. The following trend is observed. On increasing the number of carbons in the alkyl tail there is a transition from a complex phase behavior to a simple phase behavior. In all cases the transition temperatures increase with the increase of the diameter of the cation of the alkali metal (Figure 3). However, the enthalpy and entropy changes associated with the temperature transitions decrease with the increase of the cation diameter (Figure 4). At the same time both the diameters of the supramolecular columns (Figure 5) and spheres (Figure 6) increase with the increase of the cation diameter.

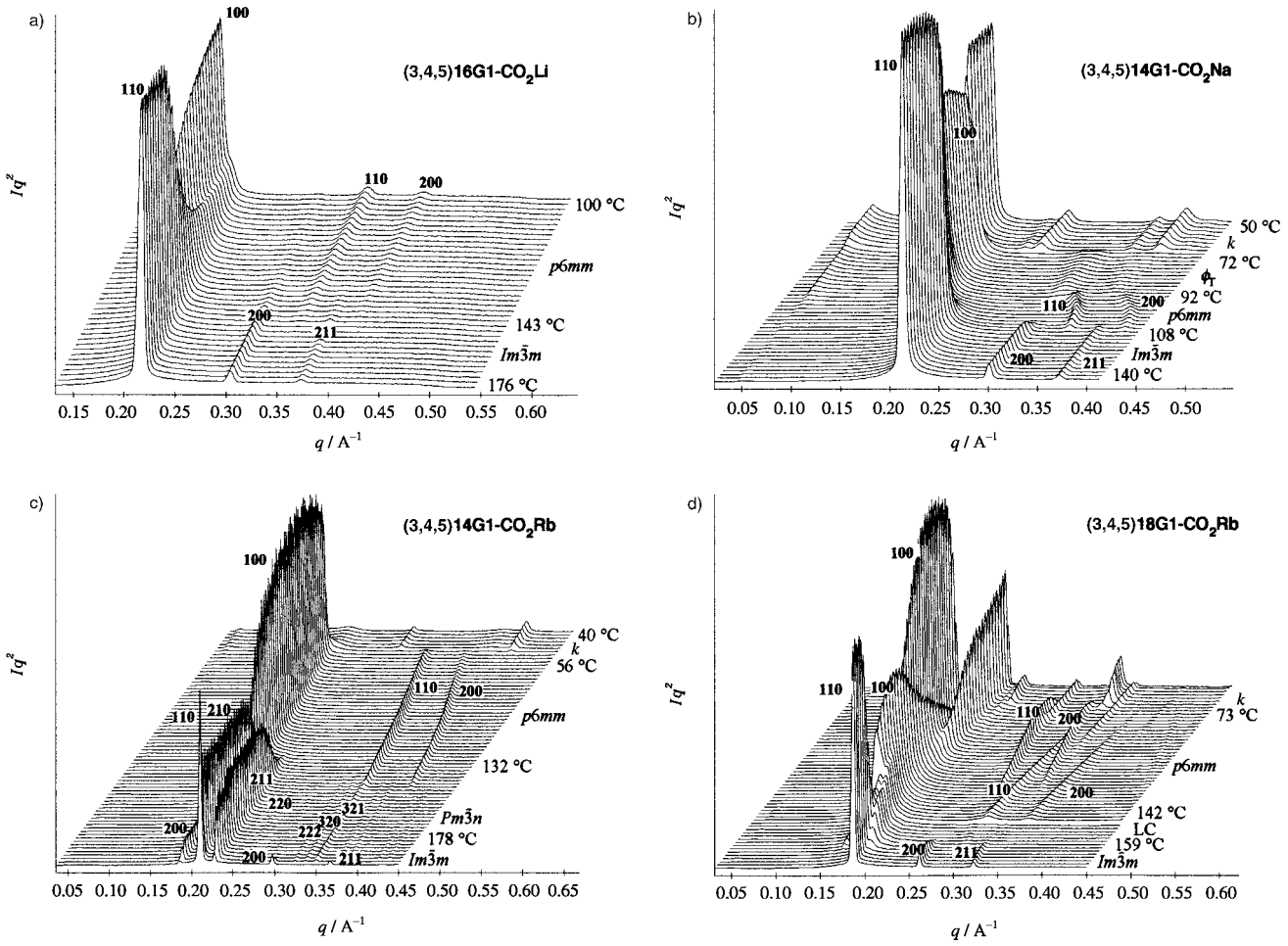

Figure 2. Selected examples of XRD experiments recorded as a function of temperature for **(3,4,5)*n*G1-CO_2M**: a) **(3,4,5)16G1-CO_2Li**; b) **(3,4,5)14G1-CO_2Na**; c) **(3,4,5)14G1-CO_2Rb**; d) **(3,4,5)18G1-CO_2Rb**.

Table 2. Thermal transitions of the minidendritic carboxylate salts **(3,4,5)12G1-CO_2M**.

M	Thermal transitions [°C] and corresponding enthalpy changes [kcal mol^{-1}][a]	
	Heating	Cooling
Li	k[b] 63.65 (16.10) Φ_h[c] 129.70 (3.23) $Im\bar{3}m$[d] dec[e]	dec $Im\bar{3}m$ 92.34 (1.08) Φ_h −5.32 (4.72) k
	k 1.6 (3.20) Φ_h 127.00 (1.09) $Im\bar{3}m$ dec	
Na	k 47.78 (6.27) Φ_r[f] 96.80 (1.35) Φ_h 119.15 (1.20) $Pm\bar{3}n$[g] 165 $Im\bar{3}m$[h] dec	dec $Im\bar{3}m$[h] 165 $Pm\bar{3}n$ 99.97 (1.15) Φ_h −5.99 (2.37) k
	k 2.8 (2.90) Φ_r 96.03 (2.62) Φ_h 118.82 (1.25) $Pm\bar{3}n$ 165 $Im\bar{3}m$[h] dec	
K	k 38.33 (10.72) Φ_h 122.00 (0.80) LC[h, i] 166 $Pm\bar{3}n$ 210 $Im\bar{3}m$[h] dec	dec $Im\bar{3}m$[h] 210 $Pm\bar{3}n$ 96.70 (0.52) Φ_h −12.7 (2.58) k
	k −4.5 (2.56) Φ_h 121.90 (0.60) $Pm\bar{3}n$ 210 $Im\bar{3}m$[h] dec	
Rb	k 47.37 (11.11) Φ_h 138.50 (0.62) $Pm\bar{3}n$ 200 $Im\bar{3}m$[h] dec	dec $Im\bar{3}m$[h] 200 $Pm\bar{3}n$ 125.90 (0.46) Φ_h −11.8 (3.08) k
	k −0.96 (3.23) Φ_h 141.90 (0.59) $Pm\bar{3}n$ 200 $Im\bar{3}m$[h] dec	
Cs	k 66.32 (12.54) k 118.80 (1.68) Φ_h 168.00 (0.65) $Pm\bar{3}n$ 210 $Im\bar{3}m$[h] dec	dec $Im\bar{3}m$[h] 210 $Pm\bar{3}n$ 162.50 (0.37) Φ_h −9.24 (3.08) k
	k 3.00 (3.45) Φ_h 171.60 (0.58) $Pm\bar{3}n$ 210 $Im\bar{3}m$[h] dec	

[a] Data from the first heating and cooling scans are given in the first line; data from the second heating are on the second line. [b] k = crystalline lattice. [c] $\Phi_h = p6mm$ hexagonal columnar lattice. [d] $Im\bar{3}m$ cubic lattice. [e] dec = decomposition temperature. [f] $\Phi_r = c2mm$ rectangular columnar lattice. [g] $Pm\bar{3}n$ cubic lattice. [h] Lattice observed only by XRD. [i] LC = unidentified liquid crystalline lattice.

Table 3. Thermal transitions of the minidendritic carboxylate salts **(3,4,5)14G1-CO_2M**.

M	Thermal transitions [°C] and corresponding enthalpy changes [kcal mol^{-1}][a]	
	Heating	Cooling
Li	k[b] 73.31 (17.72) Φ_h[c] 118.00 (1.61) $Im\bar{3}m$[d] dec[e]	dec $Im\bar{3}m$ 82.60 (1.25) Φ_h 19.22 (8.56) k
	k 29.04 (7.93) Φ_h 118.20 (1.39) $Im\bar{3}m$ dec	
Na	k 64.04 (13.55) Φ_r[f] 66.9 (6.78) Φ_h 112.40 (1.62) $Im\bar{3}m$ dec	dec $Im\bar{3}m$ 90.52 (1.40) Φ_h 16.9 (7.04) k
	k 26.00 (7.50) Φ_r 92.30 (0.16) Φ_h 111.30 (1.55) $Im\bar{3}m$ dec	
K	k 44.24 (10.98) Φ_h 97.50 (6.84) LC[g] 117.36 (0.72) $Im\bar{3}m$ dec	dec $Im\bar{3}m$ 93.56 (0.89) Φ_h 14.26 (6.33) k
	k 28.70 (6.57) Φ_h 117.50 (0.60) $Im\bar{3}m$ dec	
Rb	k 49.15 (18.98) Φ_h 127.50 (1.63) $Pm\bar{3}n$[h] 178 $Im\bar{3}m$[i] dec	dec $Im\bar{3}m$[i] 178 $Pm\bar{3}n$ 120.60 (0.75) Φ_h 17.66 (6.57) k
	k 32.60 (6.09) Φ_h 135.30 (0.82) $Pm\bar{3}n$ 178 $Im\bar{3}m$[i] dec	
Cs	k 67.37 (17.75) Φ_h 142.80 (1.56) $Pm\bar{3}n$ 204 $Im\bar{3}m$[i] dec	dec $Im\bar{3}m$[i] 204 $Pm\bar{3}n$ 145.10 (0.63) Φ_h 20.84 (6.75) k
	k 39.36 (6.79) Φ_h 153.70 (0.75) $Pm\bar{3}nm$ 204 $Im\bar{3}m$[i] dec	

[a] Data from the first heating and cooling scans are on the first line; data from the second heating are on the second line. [b] k = crystalline lattice. [c] $\Phi_h = p6mm$ hexagonal columnar lattice. [d] $Im\bar{3}m$ cubic lattice. [e] dec = decomposition temperature. [f] $\Phi_r = c2mm$ rectangular columnar lattice. [g] LC = unidentified liquid crystalline lattice. [h] $Pm\bar{3}n$ cubic lattice. [i] Lattice observed only by XRD.

Table 4. Thermal transitions of the minidendritic carboxylate salts **(3,4,5)16G1-CO_2M**.

M	Thermal transitions [°C] and corresponding enthalpy changes [kcal mol^{-1}][a]	
	Heating	Cooling
Li	k[b] 58.49 (29.63) Φ_h[c] 106.10 (1.98) $Im\bar{3}m$[d] dec[e]	dec $Im\bar{3}m$ 83.01 (1.30) Φ_h 37.44 (10.54) k
	k 41.10 (15.09) Φ_h 107.20 (1.45) $Im\bar{3}m$ dec	
Na	k 76.81 (24.59) k 90.00 (2.31) Φ_h 106.22 (1.62) $Im\bar{3}m$ dec	dec $Im\bar{3}m$ 81.13 (1.50) Φ_h 31.52 (10.76) k
	k 45.78 (11.11) k 76.50 (0.06) Φ_h 105.10 (1.65) $Im\bar{3}m$ dec	
K	k 58.84 (19.81) Φ_h 111.36 (1.32) LC[f, g] 138 $Im\bar{3}m$ dec	dec $Im\bar{3}m$ 123.75 (0.89) Φ_h 36.33 (9.96) k
	k 52.70 (9.53) Φ_h 111.05 (1.35) $Im\bar{3}m$ dec	
Rb	k 59.21 (23.59) Φ_h 125.30 (0.71) LC[g] 153 $Im\bar{3}m$ dec	dec $Im\bar{3}m$ 123.75 (0.89) Φ_h 36.33 (9.96) k
	k 55.22 (10.89) Φ_h 133.91 (1.09) $Im\bar{3}m$ dec	
Cs	k 62.82 (11.54) k 75.00 (13.25) Φ_h 142.80 (1.02) $Pm\bar{3}n$[h] 200 $Im\bar{3}m$[g] dec	dec $Im\bar{3}m$[g] 200 $Pm\bar{3}n$ 137.05 (0.71) Φ_h 39.31 (12.26) k
	k 56.40 (12.65) Φ_h 146.16 (0.83) $Pm\bar{3}n$ 200 $Im\bar{3}m$[g] dec	

[a] Data from the first heating and cooling scans are on the first line; data from the second heating are on the second line. [b] k = crystalline lattice. [c] $\Phi_h = p6mm$ hexagonal columnar lattice. [d] $Im\bar{3}m$ cubic lattice. [e] dec = decomposition temperature. [f] LC = unidentified liquid crystalline lattice. [g] Lattice observed only by XRD. [h] $Pm\bar{3}n$ cubic lattice.

Table 5. Thermal transitions of the minidendritic carboxylate salts **(3,4,5)18G1-CO_2M**.

M	Thermal transitions [°C] and corresponding enthalpy changes [kcal mol^{-1}][a]	
	Heating	Cooling
Li	k[b] 70.24 (22.93) Φ_h[c] 106.30 (0.88) $Im\bar{3}m$[d] dec[e]	dec $Im\bar{3}m$ 79.2 (1.60) Φ_h 44.08 (16.74) k
	k 52.70 (16.37) Φ_h 105.95 (1.67) $Im\bar{3}m$ dec	
Na	k 83.67 (25.30) Φ_h 107.50 (1.80) $Im\bar{3}m$ dec	dec $Im\bar{3}m$ 84.07 (1.82) Φ_h 46.71 (16.45) k
	k 62.98 (12.79) Φ_h 106.10 (1.91) $Im\bar{3}m$ dec	
K	k 70.50 (28.54) Φ_h 107.22 (1.47) $Im\bar{3}m$ dec	dec $Im\bar{3}m$ 88.29 (1.49) Φ_h 47.42 (15.08) k
	k 64.85 (13.14) Φ_h 107.30 (1.55) $Im\bar{3}m$ dec	
Rb	k 71.46 (19.47) Φ_h 126.50 (2.01) LC[f, g] 159 $Im\bar{3}m$ dec	dec $Im\bar{3}m$ 110.90 (1.15) Φ_h 48.47 (15.90) k
	k 67.82 (14.42) Φ_h 126.50 (1.20) $Im\bar{3}m$ dec	
Cs	k 72.15 (17.22) Φ_h 110.22 (10.21) LC[g] 174 $Im\bar{3}m$ dec	dec $Im\bar{3}m$ 126.20 (0.89) Φ_h 50.33 (17.56) k
	k 68.66 (15.75) Φ_h 138.00 (0.92) $Im\bar{3}m$ dec	

[a] Data from the first heating and cooling scans are on the first line; data from the second heating are on the second line. [b] k = crystalline lattice. [c] $\Phi_h = p6mm$ hexagonal columnar lattice. [d] $Im\bar{3}m$ cubic lattice. [e] dec = decomposition temperature. [f] LC = unidentified liquid crystalline lattice. [g] Lattice observed only by XRD.

0947-6539/02/0805-1110 $ 17.50+.50/0 *Chem. Eur. J.* **2002**, *8*, No. 5

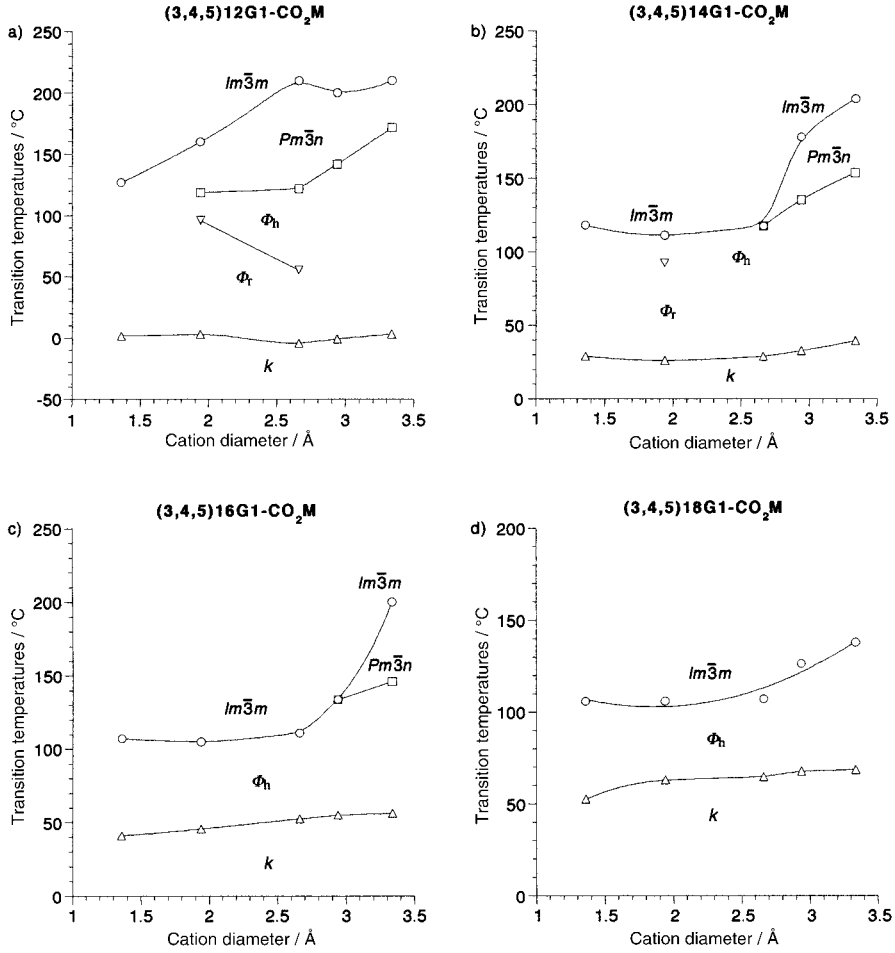

Figure 3. The dependence of transition temperatures of **(3,4,5)12G1-CO_2M** from second heating DSC scans on the cation diameter; crystalline melting (△), Φ_r to Φ_h (▽), Φ_h to $Pm\bar{3}n$ (□) and $Pm\bar{3}n$ to $Im\bar{3}m$ (○): a) **(3,4,5)12G1-CO_2M**; b) **(3,4,5)14G1-CO_2M**; c) **(3,4,5)16G1-CO_2M**; d) **(3,4,5)18G1-CO_2M** (M = Li, Na, K, Rb and Cs.

The following tentative explanation can be provided for these experimental trends. The self-assembly of the minidendritic alkali metal salts is determined by the aggregation of the metal carboxylates in the center of the supramolecular structure. The increase of the diameter of the metal from the **(3,4,5)*n*G1-CO_2M** salts decreases the strength of the interaction between the metal carboxylate ion pairs which are aggregated in the focal point of the spherical or in the center of the cylindrical supramolecular minidendrimer.

Let us discuss the temperature transition trend only on the columnar to cubic phase transition (Figures 1, 3). If the column to sphere shape transition temperature would be determined by the strength of the ion pair aggregation, we would expect the highest temperature transition at the lowest cation diameter, that is, Li. However, the highest temperature transition occurs at the highest cation diameter, that is, Cs, and therefore at the weakest ion pair

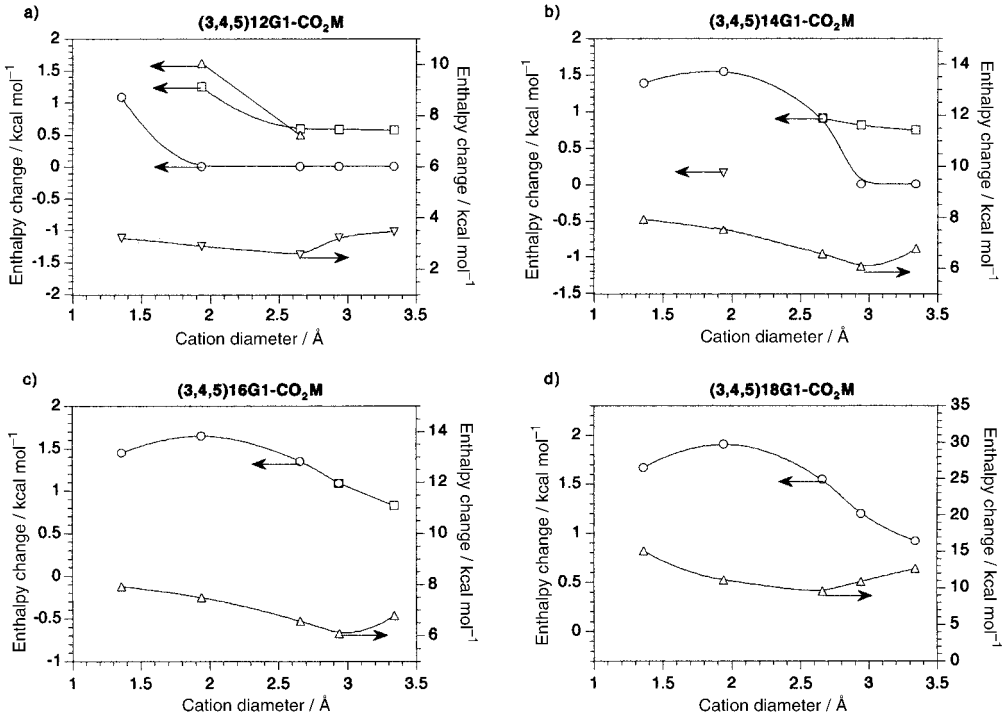

Figure 4. The dependence of enthalpy changes associated with the transition temperatures of **(3,4,5)*n*G1-CO_2M** on the cation diameter (second heating DSC scans); crystalline melting (△), Φ_r to Φ_h (▽), Φ_h to $Pm\bar{3}n$ (□) and to $Im\bar{3}m$ (○) transitions; a) **(3,4,5)12G1-CO_2M**; b) **(3,4,5)14G1-CO_2M**; c) **(3,4,5)16G1-CO_2M**; d) **(3,4,5)18G1-CO_2M** (M = Li, Na, K, Rb and Cs).

Table 6. Measured *d*-spacings of the *c2mm* rectangular columnar, *p6mm* hexagonal columnar, $Pm\bar{3}n$ and $Im\bar{3}m$ cubic lattices generated by **(3,4,5)*n*G1-CO$_2$M** ($n = 12$, 14, 16, 18, M = Li, Na, K, Rb, Cs).

Monodendron	T [°C]	Lattice	d_{100} (d_{200})[a] (d_{310})[b] [Å]	d_{110} (d_{110})[a] (d_{222})[b] [Å]	d_{200} (d_{310})[a] (d_{320})[b] [Å]	d_{210} (d_{020})[a] (d_{321})[b] [Å]	d_{211} (d_{400})[a] [Å]	d_{220} [Å]
(3,4,5)12G1-CO$_2$Li	120	*p6mm*	29.6	17.0	14.9			
	166	$Im\bar{3}m$		28.4	20.1		16.3	
(3,4,5)12G1-CO$_2$Na	68	*c2mm*	34.4[a]	33.0[a]				
	136	*p6mm*	30.7	17.8				
	156	$Pm\bar{3}n$			31.7	28.7	26.3	
	160	$Im\bar{3}m$		27.8	19.5			
(3,4,5)12G1-CO$_2$K	108	*p6mm*	32.3					
	200	$Pm\bar{3}n$			33.2	29.8	27.0	
	210	$Im\bar{3}m$		28.5	20.0			
(3,4,5)12G1-CO$_2$Rb	80	*p6mm*	33.2	19.2	16.6	12.6		
	160	$Pm\bar{3}n$			34.1	29.7	28.0	
	200	$Im\bar{3}m$		28.4	19.9		16.2	
(3,4,5)12G1-CO$_2$Cs	100	*p6mm*	32.6	18.7	16.2			
	160	$Pm\bar{3}n$			33.2	29.1	27.0	
	210	$Im\bar{3}m$		28.1	19.8		16.2	
(3,4,5)14G1-CO$_2$Li	105	*p6mm*	29.6	17.3	14.8			
	140	$Im\bar{3}m$		28.4	20.3		165	
(3,4,5)14G1-CO$_2$Na	68	*c2mm*	36.4[a, c]	36.4[a,c]	21.2[a]	20.6[a]		
	96	*p6mm*	34.0	19.6	16.9			
	140	$Im\bar{3}m$		29.5	20.9		16.9	
(3,4,5)14G1-CO$_2$K	100	*p6mm*	34.7	19.9	17.3			
	170	$Im\bar{3}m$		29.6	20.9		17.0	
(3,4,5)14G1-CO$_2$Rb	100	*p6mm*	36.7	21.2	18.2			
	160	$Pm\bar{3}n$			34.3	30.7	28.0	24.5
			21.8[b]	19.9[b]	19.1[b]	18.3[b]	17.1[b]	
	180	$Im\bar{3}m$		29.9	21.2		17.1	
(3,4,5)14G1-CO$_2$Cs	110	*p6mm*	34.3	19.6	17.0			
	160	$Pm\bar{3}n$			36.2	32.3	29.5	
	228	$Im\bar{3}m$		29.9	21.0		17.1	
(3,4,5)16G1-CO$_2$Li	100	*p6mm*	31.4	18.2	15.7			
	176	$Im\bar{3}m$		29.0	20.6		16.8	
(3,4,5)16G1-CO$_2$Na	81	*p6mm*	35.6	20.7	17.8	13.3		
	111	$Im\bar{3}m$		30.8	21.7		17.7	
(3,4,5)16G1-CO$_2$K	90	*p6mm*	37.0	21.5	18.6	13.8		
	150	$Im\bar{3}m$		32.1	22.7		18.6	
(3,4,5)16G1-CO$_2$Rb	105	*p6mm*	36.9	21.4	18.5			
	165	$Im\bar{3}m$		31.8	22.7	18.4	15.8	
(3,4,5)16G1-CO$_2$Cs	105	*p6mm*	37.3	21.7	19.0			
	190	$Im\bar{3}m$			36.9	32.9	30.0	
	200	$Im\bar{3}m$		31.9	22.7		18.4	
(3,4,5)18G1-CO$_2$Li	110	*p6mm*	33.0	19.1	16.5			
	150	$Im\bar{3}m$		31.0	21.8		17.8	
(3,4,5)18G1-CO$_2$Na	100	*p6mm*	36.2	20.8	18.0			
	135	$Im\bar{3}m$		31.8	22.4		18.3	
(3,4,5)18G1-CO$_2$K	100	*p6mm*	38.7	22.3	19.3			
	135	$Im\bar{3}m$		33.7	23.8		19.3	
(3,4,5)18G1-CO$_2$Rb	122	*p6mm*	38.4	22.3	19.2			
	170	$Im\bar{3}m$		33.7	24.0		19.5	
(3,4,5)18G1-CO$_2$Cs	90	*p6mm*	40.4	23.5	20.3			
	190	$Im\bar{3}m$		33.8	27.8		19.4	

[a] *d*-Spacings for [a] *c2mm* rectangular hexagonal and [b] $Pm\bar{3}n$ cubic lattices. [c] Overlapping peaks.

interaction. Therefore, most probably the higher temperature transition is determined by the higher diameter of the column (Figure 5). Due to the weaker aggregation of the ion pair, the column with larger diameters should exhibit a lower enthalpy change associated with their higher columnar–cubic transition temperature. As observed from the results plotted in Figure 4, this is indeed the case.

Table 7. Structural analysis by XRD of the two-dimensional *c2mm* rectangular and *p6mm* hexagonal columnar lattices formed by the self-organization of the cylindrical supramolecular dendrimers self-assembled from **(3,4,5)*n*G1-CO$_2$M**.

M	**n**	T [°C]	Lattice	$\langle d_{100}\rangle$[a] [Å]	a[a] (a:b)[b] [Å]	ρ_{20}[c] [g mL^{-1}]	D[d] (C:D)[e] [Å]	μ	α'[h] [°]
Na	12	68	*c2mm*		68.9:37.6[b]	1.02	39.8:37.6[e]	5[f]	72.0
	14	68	*c2mm*		72.8:41.2[b]	1.03	42.0:41.2[e]	6[f]	60.0
Li	12	120	*p6mm*	29.6	34.2[a]	1.02	34.2[d]	4[g]	90.0
	14	105	*p6mm*	29.7	34.3[a]	1.03	34.3[d]	4[g]	90.0
	16	100	*p6mm*	31.4	36.3[a]	1.02	36.3[d]	4[g]	90.0
	18	110	*p6mm*	33.0	38.1[a]	1.00	38.1[d]	4[g]	90.0
Na	12	136	*p6mm*	30.8	35.6[a]	1.02	35.6[d]	5[g]	72.0
	14	96	*p6mm*	33.9	39.1[a]	1.03	39.1[d]	5[g]	72.0
	16	81	*p6mm*	35.6	41.1[a]	1.02	41.1[d]	5[g]	72.0
	18	100	*p6mm*	36.1	41.7[a]	1.00	41.7[d]	5[g]	90.0
K	12	108	*p6mm*	32.3	37.3[a]	1.02	37.3[d]	5[g]	72.0
	14	100	*p6mm*	34.6	40.0[a]	1.03	40.0[d]	5[g]	72.0
	16	90	*p6mm*	37.0	42.7[a]	1.02	42.7[d]	5[g]	72.0
	18	100	*p6mm*	38.6	44.6[a]	1.03	44.6[d]	5[g]	72.0
Rb	12	80	*p6mm*	33.3	38.5[a]	1.02	38.5[d]	5[g]	72.0
	14	60	*p6mm*	36.6	42.3[a]	1.03	42.3[d]	5[g]	72.0
	16	105	*p6mm*	37.0	42.7[a]	1.01	42.7[d]	5[g]	72.0
	18	122	*p6mm*	38.5	44.5[a]	1.04	44.5[d]	5[g]	72.0
Cs	12	100	*p6mm*	32.5	37.5[a]	1.02	37.5[d]	4[g]	90.0
	14	110	*p6mm*	34.1	39.4[a]	1.03	39.4[d]	4[g]	90.0
	16	105	*p6mm*	37.6	43.4[a]	1.2	43.4[d]	5[g]	72.0
	18	90	*p6mm*	40.6	46.9[a]	1.03	46.9[d]	5[g]	72.0

[a] *p6mm* hexagonal columnar lattice parameter $a = 2 < d_{100} > /\sqrt{3}$; $< d_{100} > = (d_{100} + \sqrt{3}d_{110} + \sqrt{4}d_{200} + \sqrt{7}d_{210})/4$. [b] *c2mm* rectangular columnar lattice parameters a and b (see Scheme 1). [c] Experimental density at 20 °C. [d] Experimental column diameter of *p6mm* hexagonal columnar lattice $D = 2 < d_{100} > /\sqrt{3}$. [e] Experimental elliptical column diameters of *c2mm* rectangular columnar latticecs $C = a\sqrt{3}/3$ and $D = b$ (see Scheme 1). [f] Number of monodendrons per elliptical column layer $\mu = (N_A abt\rho)/2M$. [g] Number of monodendrons per column layer $\mu = (\sqrt{3}N_A a^2 t\rho)/2M$ (Avogadro's number $N_A = 6.022045 \times 10^{23}$ mol^{-1}, the average height of the column layer $t = 4.7$ Å, M = molecular weight of minimonodendron). [h] Projection of the solid angle of the tapered and conical minimonodendrons $\alpha' = 360/\mu$ [°].

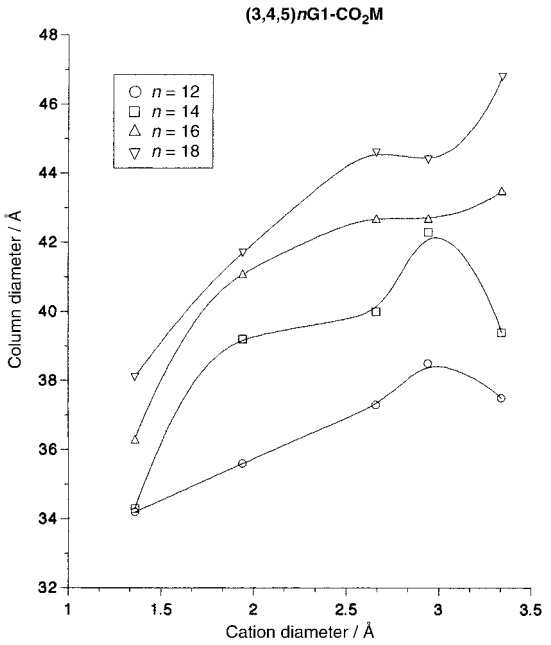

Figure 5. The dependence of the diameter of the supramolecular cylinders on the cation diameter of **(3,4,5)*n*G1-CO$_2$M** ($n = 12$, 14, 16 and 18) in their *p6mm* lattice.

0947-6539/02/0805-1112 $ 17.50+.50/0 *Chem. Eur. J.* **2002**, *8*, No. 5

Table 8. Structural analysis by XRD of the three-dimensional cubic $Pm\bar{3}n$ and $Im\bar{3}m$ lattices formed by the self-organization of the spherical supramolecular minidendrimers self-assembled from **(3,4,5)*n*G1-CO$_2$M**.

M	*n*	*T* [°C]	Lattice	ρ_{20}[a] [g mL^{-1}]	*a*[b] [Å]	*D*[c] [Å]	μ[d]	α'[e] [°]
Li	12	166	$Im\bar{3}m$	1.02	40.2	39.6	29	12.4
	14	140	$Im\bar{3}m$	1.03	40.4	39.8	27	13.3
	16	176	$Im\bar{3}m$	1.02	41.1	40.5	25	14.4
	18	150	$Im\bar{3}m$	1.00	43.7	43.0	27	13.3
Na	12	156	$Pm\bar{3}n$	1.02	64.0	39.7	29	12.4
		160	$Im\bar{3}m$	1.02	39.2	38.6	27	13.3
	14	140	$Im\bar{3}m$	1.03	41.6	41.0	29	12.4
	16	111	$Im\bar{3}m$	1.02	43.4	42.7	29	12.4
	18	135	$Im\bar{3}m$	1.00	44.9	44.2	29	12.4
K	12	200	$Pm\bar{3}n$	1.02	66.4	41.2	32	11.3
		210	$Im\bar{3}m$	1.02	40.2	39.6	28	12.9
	14	170	$Im\bar{3}m$	1.03	41.8	41.2	28	12.9
	16	150	$Im\bar{3}m$	1.02	45.5	44.8	33	10.9
	18	135	$Im\bar{3}m$	1.03	47.5	46.8	34	10.6
Rb	12	160	$Pm\bar{3}n$	1.02	67.7	42.0	31	11.6
		200	$Im\bar{3}m$	1.02	39.9	39.3	26	13.9
	14	160	$Pm\bar{3}n$	1.03	68.8	42.7	30	12.0
		180	$Im\bar{3}m$	1.03	42.2	41.6	28	12.9
	16	165	$Im\bar{3}m$	1.01	42.6	42.0	25	14.4
	18	170	$Im\bar{3}m$	1.04	47.8	47.1	34	10.6
Cs	12	160	$Pm\bar{3}n$	1.02	65.9	40.9	27	13.3
		210	$Im\bar{3}m$	1.02	39.7	39.1	24	15.0
	14	160	$Pm\bar{3}n$	1.03	72.3	44.9	33	10.9
		228	$Im\bar{3}m$	1.03	42.1	41.5	26	13.9
	16	190	$Pm\bar{3}n$	1.02	73.6	45.7	31	11.6
		200	$Im\bar{3}m$	1.02	45.2	44.5	29	12.4
	18	190	$Im\bar{3}m$	1.03	50.3	49.5	37	9.7

[a] Experimental density at 20 °C. [b] $Pm\bar{3}n$ or $Im\bar{3}m$ cubic lattice parameter, $a=(\sqrt{2}d_{110}+\sqrt{4}d_{200}+\sqrt{5}d_{210}+\sqrt{6}d_{211}+\sqrt{8}d_{220}+\sqrt{10}d_{310}+\sqrt{12}d_{222}+\sqrt{13}d_{320}+\sqrt{14}d_{321}+\sqrt{16}d_{400}+\sqrt{20}d_{420}+\sqrt{21}d_{421})/p$ (p = number of observed reflections). [c] Experimental spherical diameter $D=2\sqrt[3]{3a^3/32\pi}$ for $Pm\bar{3}n$ and $D=2\sqrt[3]{3a^3/8\pi}$ for $Im\bar{3}m$. [d] Number of monodendrons per spherical dendrimer $\mu=(a^3N_A\rho)/8M$ for $Pm\bar{3}n$ and $\mu=(a^3N_A\rho)/2M$ for $Im\bar{3}m$. [e] Projection of the solid angle of the tapered and conical minimonodendron $\alpha'=360/\mu$ [°].

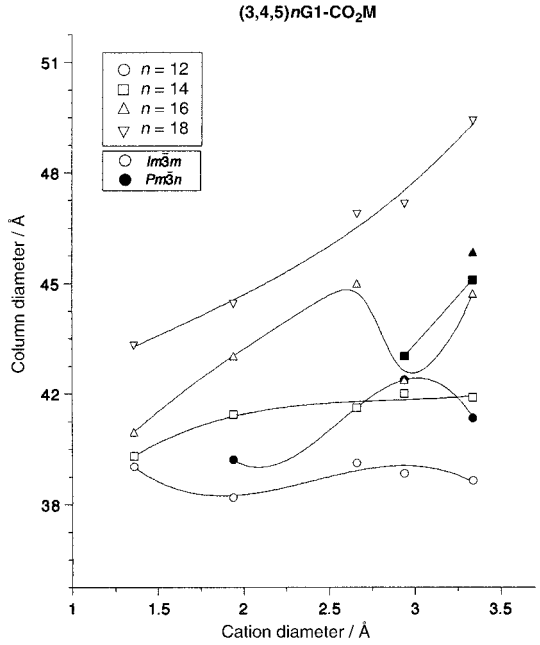

Figure 6. The dependence of the diameter of the supramolecular spheres as a function of cation diameter of **(3,4,5)*n*G1-CO$_2$M** in their cubic $Pm\bar{3}n$ and $Im\bar{3}m$ lattices; a) **(3,4,5)12G1-CO$_2$M**; b) **(3,4,5)14G1-CO$_2$M**; c) **(3,4,5)16G1-CO$_2$M**; d) **(3,4,5)18G1-CO$_2$M**.

The second place where the size of the cation and therefore the strength of the ion pair aggregation is important is in the determination of the columnar and cubic lattice symmetry. This lattice symmetry is determined by the shape of the supramolecular cylinder or sphere that determines it. At the present time we can not explain why only the sodium salts **(3,4,5)12G1-CO$_2$Na** and **(3,4,5)14G1-CO$_2$Na** form the *c2mm* rectangular columnar lattice while all other salts exhibit only the *p6mm* hexagonal columnar lattice. The rectangular columnar lattice is generated from distorted ellipsoidal cylinders or rectangular column while the hexagonal columnar lattice is produced from undistorted cylinders (Scheme 1). A detailed analysis of the *c2mm* lattice by a combination of electron density, electron diffraction, and transition electron microscopy experiments is in progress. Nevertheless we can provide at least a qualitative explanation for the formation of $Im\bar{3}m$ versus $Pm\bar{3}n$ or the combination of $Pm\bar{3}n$ and $Im\bar{3}m$ lattices for different metal salts and number of methylene units in the alkyl tail (Figure 1). As suggested in recent publications,[2b, 14] the $Im\bar{3}m$ lattice is generated from more perfect supramolecular spherical objects than the one that generates the $Pm\bar{3}n$ lattice. In the cubic lattice the alkyl tails of the supramolecular dendrimer are conformationally disordered.[9] The degree of conformational disorder of the spherical object from the cubic lattice is higher than in the columnar lattice. This difference explains the reentrant character (i.e., the two- to three-dimensional phase transition on increasing the temperature) of the columnar to cubic transition. Even if the order in the cubic lattice is three-dimensional and in the columnar lattice is two-dimensional, due to the higher conformational disorder of the spherical objects the overall entropy is higher in the three-dimensional lattice than in the two-dimensional lattice. This can explain the "apparent against" thermodynamic character of the columnar to cubic phase transition. As we can see from Figure 1 a–c the smallest alkali metal salts produce the most perfect spheres directly from the cylinders, that is, **(3,4,5)12G1-CO$_2$Li** forms the $Im\bar{3}m$ cubic phase. Most probably this is due to the highest interaction at the focal point of the sphere. The **(3,4,5)12G1-CO$_2$M** with M = Na, K, Rb and Cs require the formation of the $Pm\bar{3}n$ lattice that is generated from less perfect spheres before the $Im\bar{3}m$ lattice forms. Obviously, a stronger interaction in the core of the sphere allows to create at the same temperature a higher degree of conformational disorder and therefore, a more perfect sphere. By increasing the number of carbons in the alkyl tail of the minidendron we can increase the number of conformers required to create a more perfect sphere even with larger alkali metal salts. That is, while in the case of **(3,4,5)12G1-CO$_2$M** only Li produces directly the $Im\bar{3}m$ lattice, in the case of **(3,4,5)14G1-CO$_2$M**, Li, Na and K produce directly the $Im\bar{3}m$ lattice. In the case of **(3,4,5)16G1-CO$_2$M** only Cs does not produce directly the $Im\bar{3}m$ lattice. At the same time **(3,4,5)18G1-CO$_2$M** produces only the $Im\bar{3}m$ lattice regardless of the nature of the alkali metal used.

The trends learned from this library of minidendritic alkali metal salts are extremely important because they teach us how to design larger generations of dendrimers exhibiting more perfect spherical shapes than previously observed. We should recall that previously we have encountered, with one single exception, only the $Pm\bar{3}n$ lattice in larger generations of supramolecular dendrimers.[1]

At the same time, the experiments described here are suggesting that we should expect the formation of ovoidal distorted supramolecular cylindrical dendrimers at higher generations. Previously we have encountered only the cylindrical supramolecular shapes.[1, 3]

As expected both for the case of cylindrical and spherical supramolecular minidendrons, their diameter increases by increasing the number of methylene units in their alkyl tail. This is illustrated by the plot of the a^2 in the case of the cylindrical ($p6mm$) and a^3 in the case of spherical ($Im\bar{3}m$) supramolecular minidendrimers as a function of the number of methylenic units n (Figures 7, 8).

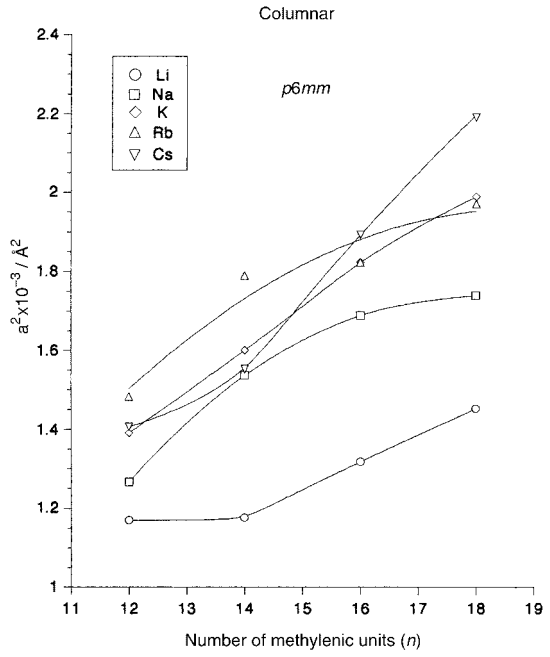

Figure 7. The dependence of the cross-section area of the cylindrical supramolecular assembly formed by **(3,4,5)*n*G1-CO$_2$M** as a function of n: M = a) Li; b) Na; c) K; d) Rb; e) Cs.

The elaboration of new structural concepts in the field of supramolecular dendrimers with the aid of the minidendritic models discussed here will expand the fundamental and technologic capabilities of this class of complex molecules.[15] In addition metal salts based concepts as those already elaborated both with minidendritic[16] as well as with larger generations of dendrimers[17] will be elucidated and/or developed. AB_2 and AB_3 architectural building blocks related to **(3,4,5)12G1-CO$_2$M** have been previously used in the design of other functional self-organized systems.[18] The results discussed here may also contribute to the design of novel assemblies, lattices and concepts based on the previously reported systems.[18]

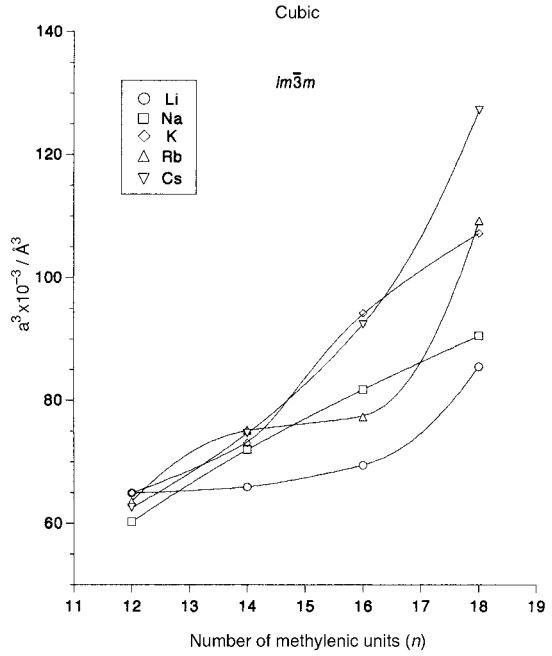

Figure 8. The dependence of the volume of the spherical supramolecular assemblies formed by **(3,4,5)*n*G1-CO$_2$M** as a function of n: M = a) Li; b) Na; c) K; d) Rb; e) Cs.

Conclusion

The synthesis of the alkali metal salts of 3,4,5-tris(n-alkan-1-yloxy)benzoic acid [**(3,4,5)*n*G1-CO$_2$M**, where n is the number of methylene units in the alkan group with $n = 12$, 14, 16, 18 and M = Li, Na, K, Rb, Cs] and the structural analysis of their supramolecular assemblies was described. All compounds self-assemble at low temperatures into supramolecular cylinders that self-organize in two-dimensional $c2mm$ rectangular columnar and/or $p6mm$ hexagonal columnar lattices. The $c2mm$ rectangular columnar lattice was not observed previously in supramolecular dendrimers. At high temperatures the same compounds self-assemble into supramolecular spheres that self-organize into three-dimensional $Pm\bar{3}n$ and/or $Im\bar{3}m$ cubic lattices. The dependence between the molecular structure of **(3,4,5)*n*G1-CO$_2$M** and the shape of the corresponding supramolecular object, lattice symmetry and the transition temperature between different lattices was established. All **(3,4,5)*n*G1-CO$_2$Li** form Φ_h and $Im\bar{3}m$ phases. Only **(3,4,5)*n*G1-CO$_2$Na** with $n = 12$ and 14 form Φ_r followed by Φ_h, $Pm\bar{3}n$ and $Im\bar{3}m$ (when $n = 12$) and Φ_h and $Im\bar{3}m$ phases (when $n = 14$). When M = K, Rb and Cs **(3,4,5)12G1-CO$_2$M** form Φ_h followed by $Pm\bar{3}n$ and $Im\bar{3}m$ lattices. By increasing n the tendency to form only Φ_h and $Im\bar{3}m$ cubic lattices increases. The only **(3,4,5)14G1-CO$_2$M** with M = Rb and Cs and **(3,4,5)16G1-CO$_2$Cs** form the sequence Φ_h, $Pm\bar{3}n$, and $Im\bar{3}m$ lattices. All other compounds exhibit Φ_h and $Im\bar{3}m$ lattices. **(3,4,5)*n*G1-CO$_2$M** represents an AB_3 minidendritic model for the larger generations of self-assembling monodendrons and therefore, the results reported here will enable the rational design of larger generations of monodendrimers which self-assemble into nanoscale supramolecular soft objects. The temperature responsive shape change of these

0947-6539/02/0805-1114 $ 17.50+.50/0 *Chem. Eur. J.* **2002**, *8*, No. 5

supramolecular soft objects and lattices are expected to contribute to the elaboration of new concepts in the field of supramolecular chemistry.

Experimental Section

Materials: Benzene (Fisher, ACS reagent) was shaken with concentrated H_2SO_4, washed twice with H_2O, dried over $MgSO_4$ and finally distilled over sodium/benzophenone. MeOH, EtOH, H_2SO_4, $MgSO_4$, and DMF (all Fisher, ACS reagents) were used as received. 1-Bromotetradecane (97%), 1-bromohexadecane (98%) (all from Lancaster) were used as received. 1-Bromododecane (98%), 1-bromooctadecane (96%), LiOH (98+%), NaOH (97+%, ACS reagent), KOH (85%, ACS reagent), RbOH (99%, 50% wt in H_2O) and CsOH (99%, 50% wt in H_2O) (all from Aldrich) were used as received.

Techniques: ^{1}H NMR (200 MHz or 500 MHz) and ^{13}C NMR (50 MHz or 125 MHz) spectra were recorded on a Varian Gemini 200 or on a Bruker DRX-500, respectively. $CDCl_3$ was used as solvent and TMS as internal standard unless otherwise noted. Chemical shifts are reported as δ, ppm. The purity of products was determined by a combination of techniques including thin-layer chromatography (TLC) on silica gel coated aluminium plates (Kodak) with fluorescent indicator and HPLC using a Perkin–Elmer Series 10 high pressure liquid chromatograph equipped with an LC-100 column oven, Nelson Analytical 900 Series integrator data station and two Perkin–Elmer PL gel columns of 5×10^2 and 1×10^4 Å. THF was used as solvent at the oven temperature of 40 °C. Detection was by UV absorbance at 254 nm.

Thermal transitions of samples that were freeze-dried from benzene were measured on a Perkin–Elmer DSC-7 differential scanning calorimeter (DSC). In all cases, the heating and cooling rates were 10 °C per min. First-order transition temperatures were reported as the maxima and minima of their endothermic and exothermic peaks. Indium and zinc were used as calibration standards. An Olympus BX-40 optical polarized microscope (100× magnification) equipped with a Mettler FP 82 hot stage and a Mettler FP 80 central processor was used to verify thermal transitions and characterize anisotropic textures.

X-ray diffraction (XRD) experiments on liquid crystal phases were performed by using either a helium-filled flat plate wide angle (WAXS) camera or a pinhole-collimated small angle (SAXS) camera, and also by using an Image Plate area detector (MAR Research) with a graphite-monochromatized a pinhole-collimator beam and a helium tent. The samples, in glass capillaries, were held in a temperature-controlled cell (±0.1 °C). Ni-filtered $Cu_{K\alpha}$ radiation was used. Experiments were also performed at several small-angle stations of the synchrotron radiation source at Daresbury (UK). A double-focused beam and a quadrant detector were used. In both cases, the sample was held in a capillary within a custom-built temperature cell controlled to within ±0.1 °C. Capillaries of the dried carboxylate salts were sealed under nitrogen. Densities, ρ, were determined by flotation in glycerol/H_2O or glycerol/MeOH.

Synthesis

Methyl [3,4,5-tris(*n*-alkan-1-yloxy)]benzoates [(3,4,5)*n*G1-CO_2CH_3] were synthesized by standard techniques used in our laboratory for the synthesis of **(3,4,5)*n*G1-CO_2CH_3**.[1, 3b]

Methyl [3,4,5-tris(*n*-dodecan-1-yloxy)]benzoate [(3,4,5)12G1-CO_2CH_3][3b] was synthesized by standard techniques used in our laboratories.

Methyl [3,4,5-tris(*n*-tetradecan-1-yloxy)]benzoate [(3,4,5)14G1-CO_2CH_3]: purity (GPC): 99+%; $R_f = 0.31$ (hexane/ethyl acetate 20:1); ^{1}H NMR ($CDCl_3$, TMS): $\delta = 0.88$ (t, $J = 6.3$ Hz, 9H, CH_3), 1.26 (m, 60H, $CH_3(CH_2)_{10}$), 1.46 (m, 6H, CH_2CH$_2$CH$_2$OAr), 1.77 (m, 6H, CH_2CH$_2$OAr), 3.89 (s, 3H, CO_2CH_3), 4.01 (t, $J = 6.3$ Hz, 6H, CH_2OAr), 7.25 (s, 2H, ArHCO$_2$CH$_3$); ^{13}C NMR ($CDCl_3$, TMS): $\delta = 14.3$(*C*H$_3$), 22.9 (CH$_3$*C*H$_2$), 26.3 (*C*H$_2$CH$_2$CH$_2$OAr), 29.6 (CH$_3$(CH$_2$)$_2$*C*H$_2$), 29.9 (CH$_3$(CH$_2$)$_3$(*C*H$_2$)$_7$), 30.5 (*C*H$_2$CH$_2$OAr), 32.2 (CH$_3$CH$_2$*C*H$_2$), 52.3 (CO$_2$*C*H$_3$), 69.3 (*C*H$_2$OAr, 3,5-positions), 73.7 (*C*H$_2$OAr, 4-position), 108.1 (*ortho* to CO$_2$CH$_3$), 124.8 (*ipso* to CO$_2$CH$_3$), 142.5 (*para* to CO$_2$CH$_3$), 153.0 (*meta* to CO$_2$CH$_3$), 167.2 (*C*O$_2$CH$_3$); elemental analysis calcd (%) for $C_{50}H_{92}O_5$: C 77.66, H 11.99; found: C 77.71, H 11.96.

Methyl [3,4,5-tris(*n*-hexadecan-1-yloxy)]benzoate [(3,4,5)16G1-CO_2CH_3]: purity (GPC): 99+%; $R_f = 0.35$ (hexane/ethyl acetate 20:1); ^{1}H NMR ($CDCl_3$, TMS): $\delta = 0.88$ (t, $J = 6.3$ Hz, 9H, CH_3), 1.27 (m, 72H, CH$_3$(CH_2)$_{12}$), 1.46 (m, 6H, CH_2CH$_2$CH$_2$OAr), 1.80 (m, 6H, CH_2CH$_2$OAr), 3.90 (s, 3H, CO$_2$CH_3), 4.03 (t, $J = 6.3$ Hz, 6H, CH_2OAr), 7.26 (s, 2H, ArHCO$_2$CH$_3$); ^{13}C NMR ($CDCl_3$, TMS): $\delta = 14.3$ (*C*H$_3$), 22.9 (CH$_3$*C*H$_2$), 26.3 (*C*H$_2$CH$_2$CH$_2$OAr), 29.6 (CH$_3$(CH$_2$)$_2$*C*H$_2$), 29.9 (CH$_3$(CH$_2$)$_3$(*C*H$_2$)$_9$), 30.5 (*C*H$_2$CH$_2$OAr), 32.2 (CH$_3$CH$_2$*C*H$_2$), 52.3 (CO$_2$*C*H$_3$), 69.3 (*C*H$_2$OAr, 3,5-positions), 73.7 (*C*H$_2$OAr, 4-position), 108.1 (*ortho* to CO$_2$CH$_3$), 124.8 (*ipso* to CO$_2$CH$_3$), 142.5 (*para* to CO$_2$CH$_3$), 153.0 (*meta* to CO$_2$CH$_3$), 167.2 (137.8 *C*O$_2$CH$_3$); elemental analysis calcd (%) for $C_{56}H_{104}O_5$: C 77.84, H 12.23; found: C 77.81, H 12.25.

Methyl [3,4,5-tris(*n*-octadecan-1-yloxy)]benzoate [(3,4,5)18G1-CO_2CH_3]: purity (GPC): 99+%; $R_f = 0.33$ (hexane/ethyl acetate); ^{1}H NMR ($CDCl_3$, TMS): $\delta = 0.88$ (t, $J = 6.3$ Hz, 9H, CH_3), 1.26 (m, 84H, CH$_3$(CH_2)$_{10}$), 1.46 (m, 6H, CH_2CH$_2$CH$_2$OAr), 1.77 (m, 6H, CH_2CH$_2$OAr), 3.89 (s, 3H, CO$_2$CH_3), 4.01 (t, $J = 6.3$ Hz, 6H, CH_2OAr), 7.25 (s, 2H, ArHCO$_2$CH$_3$); ^{13}C NMR ($CDCl_3$, TMS): $\delta = 14.3$ (*C*H$_3$), 22.9 (CH$_3$*C*H$_2$), 26.3 (*C*H$_2$CH$_2$CH$_2$OAr), 29.6 (CH$_3$(CH$_2$)$_2$*C*H$_2$), 29.9 (CH$_3$(CH$_2$)$_3$(*C*H$_2$)$_7$), 30.5 (*C*H$_2$CH$_2$OAr), 32.2 (CH$_3$CH$_2$*C*H$_2$), 52.3 (CO$_2$*C*H$_3$), 69.3 (*C*H$_2$OAr, 3,5-positions), 73.7 (*C*H$_2$OAr, 4-position), 108.1 (*ortho* to CO$_2$CH$_3$), 124.8 (*ipso* to CO$_2$CH$_3$), 142.5 (*para* to CO$_2$CH$_3$), 153.0 (*meta* to CO$_2$CH$_3$), 167.2 (*C*O$_2$CH$_3$); elemental analysis calcd (%) for $C_{62}H_{116}O_5$: C 79.09, H 12.42; found: C 79.13, H 12.42.

General procedure for the synthesis of the alkaline salts of 3,4,5-tris(*n*-alkan-1-yloxy)benzoic acid [(3,4,5)*n*G1-CO_2M, *n* = 12, 14, 16 and 18 and M = Li, Na, K, Rb and Cs]: The syntheses of **(3,4,5)12G1-CO_2Na**, **(3,4,5)12G1-CO_2Cs**, **(3,4,5)14G1-CO_2Cs**, and **(3,4,5)16G1-CO_2Cs** were published previously,[9b] and the procedure was slightly modified for the synthesis of the other carboxylate alkali metal salts. In a 200 mL round-bottom flask equipped with magnetic stirrer and condenser, the methyl benzoate **[(3,4,5)*n*G1-CO_2CH_3]** (3.1 mmol) was dissolved in 50 to 90% EtOH (100 mL) at 95 °C. Subsequently, the correspondending alkali metal hydroxide (MOH) (15.5 mmol) was added and the mixture was stirred at reflux for 10 h. The reaction mixture was cooled to 23 °C and the precipitate was filtered under vacuum. The resulting salt was recrystallized four times from EtOH (90%) and dried under vacuum at 23 °C. Subsequently, the products were freeze-dried from benzene and stored under Ar.

(3,4,5)12G1-CO_2Li: Starting from **(3,4,5)12G1-CO_2CH_3** (2.13 g, 3.1 mmol) and LiOH (0.372 g, 15.5 mmol) in 90% EtOH (75 mL) at 95 °C for 10 h, the title compound is obtained as a white powder (1.48 g, 70.5%) after filtration followed by four recrystallizations from EtOH (90%). Purity (HPLC): 99+%; ^{1}H NMR ($CDCl_3$/[D$_6$]DMSO, 50 °C, TMS): $\delta = 0.87$ (t, $J = 6.3$ Hz, 9H, CH_3), 1.1–1.9 (overlapped, 60H, CH$_3$(CH_2)$_{10}$), 3.65 (m, 4H, 3,5-CH_2OAr), 3.79 (t, 2H, 4-CH_2OAr), 6.9 (s, 2H, Ar); ^{13}C NMR ($CDCl_3$/[D$_6$]DMSO, 50 °C, TMS): $\delta = 14.2$ (*C*H$_3$), 22.7 (CH$_3$*C*H$_2$), 25.8 (*C*H$_2$CH$_2$OAr), 28.9–30.3 (*C*H$_2$), 31.9 (CH$_3$CH$_2$*C*H$_2$), 69.2 (*C*H$_2$OAr), 108.4 (Ar-*C*2,6), 131.5 (Ar-*C*1), 135.2 (Ar-*C*4), 154.1 (Ar-*C*3,5), 176.4 (*C*OO$^-$); elemental analysis calcd (%) for $C_{43}H_{77}LiO_5$: C 75.84, H 11.40; found: C 75.56, H 11.38.

(3,4,5)12G1-CO_2K: Starting from **(3,4,5)12G1-CO_2CH_3** (2.13 g, 3.1 mmol) and KOH (0.869 g, 15.5 mmol) in 90% EtOH (75 mL) at 95 °C for 10 h, the title compound is obtained as a white powder (1.543 g, 69.9%) after filtration followed by four recrystallizations from EtOH (90%). Purity (HPLC): 99+%; ^{1}H NMR ($CDCl_3$/[D$_6$]DMSO, 50 °C, TMS): $\delta = 0.87$ (t, $J = 6.3$ Hz, 9H, CH_3), 1.1–1.9 (overlapped, 60H, CH$_3$(CH_2)$_{10}$), 3.65 (m, 4H, 3,5-CH_2OAr), 3.79 (t, 2H, 4-CH_2OAr), 6.9 (s, 2H, Ar); ^{13}C NMR ($CDCl_3$/[D$_6$]DMSO, 50 °C, TMS): $\delta = 14.2$ (*C*H$_3$), 22.7 (CH$_3$*C*H$_2$), 25.8 (*C*H$_2$CH$_2$OAr), 28.9–30.3 (*C*H$_2$), 31.9 (CH$_3$CH$_2$*C*H$_2$), 69.2 (*C*H$_2$OAr), 108.4 (Ar-*C*2,6), 131.5 (Ar-*C*1), 135.2 (Ar-*C*4), 154.1 (Ar-*C*3,5), 177.5 (*C*OO$^-$); elemental analysis calcd (%) for $C_{43}H_{77}KO_5 \times 0.5\,H_2O$: C 71.51, H 10.89; found: C 71.94, H 10.90.

(3,4,5)12G1-CO_2Rb: Starting from **(3,4,5)12G1-CO_2CH_3** (2.13 g, 3.1 mmol) and RbOH 50% wt in H_2O (1.588 g, 15.5 mmol) in 90% EtOH (75 mL) at 95 °C for 10 h, the title compound was obtained as a white powder (1.68 g, 71.5%) after filtration followed by four recrystallizations from EtOH (90%). Purity (HPLC): 99+%; ^{1}H NMR ($CDCl_3$/[D$_6$]DMSO, 50 °C, TMS): $\delta = 0.87$ (t, $J = 6.3$ Hz, 9H, CH_3), 1.1–1.9 (overlapped, 60H, CH$_3$(CH_2)$_{10}$), 3.65 (m, 4H, 3,5-CH_2OAr), 3.79 (t, 2H, 4-CH_2OAr), 6.9 (s, 2H, Ar); ^{13}C NMR ($CDCl_3$/[D$_6$]DMSO, 50 °C, TMS): $\delta = 14.2$ (*C*H$_3$), 22.7

(CH_3CH_2), 25.8 (CH_2CH_2OAr), 28.9–30.3 (CH_2), 31.9 ($CH_3CH_2CH_2$), 69.2 (CH_2OAr), 108.4 (Ar-*C*2,6), 131.5 (Ar-*C*1), 135.2 (Ar-*C*4), 154.1 (Ar-*C*3,5), 175.2 (COO^-); elemental analysis calcd (%) for $C_{43}H_{77}O_5Rb \times 0.5\,H_2O$: C 67.20, H 10.23; found: C 67.29, H 10.22.

(3,4,5)14G1-CO_2Li: Starting from **(3,4,5)14G1-CO_2CH_3** (2.39 g, 3.1 mmol) and LiOH (0.372 g, 15.5 mmol) in 90% EtOH (80 mL) at 95 °C for 10 h, the title compound was obtained as a white powder (1.71 g, 72.4%) after filtration followed by four recrystallizations from EtOH (90%). Purity (HPLC): 99+%; ^{1}H NMR ($CDCl_3$/[D_6]DMSO, 50 °C, TMS): $\delta = 0.87$ (t, $J = 6.3$ Hz, 9H, CH_3), 1.1–1.9 (overlapped, 72H, $CH_3(CH_2)_{12}$), 3.65 (m, 4H, 3,5-CH_2OAr), 3.79 (t, 2H, 4-CH_2OAr), 6.9 (s, 2H, Ar); ^{13}C NMR ($CDCl_3$/[D_6]DMSO, 50 °C, TMS): $\delta = 14.2$ (CH_3), 22.7 (CH_3CH_2), 25.8 (CH_2CH_2OAr), 28.9–30.3 (CH_2), 31.9 ($CH_3CH_2CH_2$), 69.2 (CH_2OAr), 108.4 (Ar-*C*2,6), 131.5 (Ar-*C*1), 135.2 (Ar-*C*4), 154.1 (Ar-*C*3,5), 176.4 (COO^-); elemental analysis calcd (%) for $C_{49}H_{89}LiO_5$: C 76.91, H 11.72; found: C 76.80, H 11.70.

(3,4,5)14G1-CO_2Na: Starting from **(3,4,5)14G1-CO_2CH_3** (2.39 g, 3.1 mmol) and NaOH (0.619 g, 15.5 mmol) in 90% EtOH (80 mL) at 95 °C for 10 h, the title compound was obtained as a white powder (1.76 g, 73.1%) after filtration followed by four recrystallizations from EtOH (90%). Purity (HPLC): 99+%; ^{1}H NMR ($CDCl_3$/[D_6]DMSO, 50 °C, TMS): $\delta = 0.87$ (t, $J = 6.3$ Hz, 9H, CH_3), 1.1–1.9 (overlapped, 72H, $CH_3(CH_2)_{12}$), 3.65 (m, 4H, 3,5-CH_2OAr), 3.79 (t, 2H, 4-CH_2OPh), 6.9 (s, 2H, Ar); ^{13}C NMR ($CDCl_3$/[D_6]DMSO, 50 °C, TMS): $\delta = 14.2$ (CH_3), 22.7 (CH_3CH_2), 25.8 (CH_2CH_2OAr), 28.9–30.3 (CH_2), 31.9 ($CH_3CH_2CH_2$), 69.2 (CH_2OAr), 108.4 (Ar-*C*2,6), 131.5 (Ar-*C*1), 135.2 (Ar-*C*4), 154.1 (Ar-*C*3,5), 176.8 (COO^-); elemental analysis calcd (%) for $C_{49}H_{89}NaO_5 \times 0.5\,H_2O$: C 74.48, H, 11.48; found: C 74.21, H, 11.49.

(3,4,5)14G1-CO_2K: Starting from methyl **(3,4,5)14G1-CO_2CH_3** and KOH (0.868 g, 15.5 mmol) in 90% EtOH (80 mL) at 95 °C for 10 h, the title compound was obtained as a white powder (1.79 g, 72.8%) after filtration followed by four recrystallizations from EtOH (90%). Purity (HPLC): 99+%; ^{1}H NMR ($CDCl_3$/[D_6]DMSO, 50 °C, TMS): $\delta = 0.87$ (t, $J = 6.3$ Hz, 9H, CH_3), 1.1–1.9 (overlapped, 72H, $CH_3(CH_2)_{12}$), 3.65 (m, 4H, 3,5-CH_2OAr), 3.79 (t, 2H, 4-CH_2OAr), 6.9 (s, 2H, Ar); ^{13}C NMR ($CDCl_3$/[D_6]DMSO, 50 °C, TMS): $\delta = 14.2$ (CH_3), 22.7 (CH_3CH_2), 25.8 (CH_2CH_2OAr), 28.9–30.3 (CH_2), 31.9 ($CH_3CH_2CH_2$), 69.2 (CH_2OAr), 108.4 (Ar-*C*2,6), 131.5 (Ar-*C*1), 135.2 (Ar-*C*4), 154.1 (Ar-*C*3,5), 177.4 (COO^-); elemental analysis calcd (%) for $C_{49}H_{89}KO_5 \times 0.5\,H_2O$: C 72.99, H 11.25; found: C 72.52, H 11.27.

(3,4,5)14G1-CO_2Rb: Starting from **(3,4,5)14G1-CO_2CH_3** and RbOH 50% wt in H_2O (1.588 g, 15.5 mmol) in 90% EtOH (80 mL) at 95 °C for 10 h, the title compound was obtained as a white powder (1.85 g, 70.9%) after filtration followed by four recrystallizations from EtOH (90%). Purity (HPLC): 99+%; ^{1}H NMR ($CDCl_3$/[D_6]DMSO, 50 °C, TMS): $\delta =$ 0.87 (t, $J = 6.3$Hz, 9H, CH_3), 1.1–1.9 (overlapped, 72H, $CH_3(CH_2)_{12}$), 3.65 (m, 4H, 3,5-CH_2OAr), 3.79 (t, 2H, 4-CH_2OAr), 6.9 (s, 2H, Ar); ^{13}C NMR ($CDCl_3$/[D_6]DMSO, 50 °C, TMS): $\delta = 14.2$ (CH_3), 22.7 (CH_3CH_2), 25.8 (CH_2CH_2OAr), 28.9–30.3 (CH_2), 31.9 ($CH_3CH_2CH_2$), 69.2 (CH_2OAr), 108.4 (Ar-*C*2,6), 131.5 (Ar-*C*1), 135.2 (Ar-*C*4), 154.1 (Ar-*C*3,5), 175.8 (COO^-); elemental analysis calcd (%) for $C_{49}H_{89}O_5Rb$: C 69.76, H 10.63; found: C 69.53, H 10.64.

(3,4,5)16G1-CO_2Li: Starting from **(3,4,5)16G1-CO_2CH_3** (2.65 g, 3.1 mmol) and LiOH (0.372 g, 15.5 mmol) in 90% EtOH (100 mL) at 95 °C for 10 h, the title compound was obtained as a white powder (1.78 g, 68.3%) after filtration followed by four recrystallizations from EtOH (90%). Purity (HPLC): 99+%; ^{1}H NMR ($CDCl_3$/[D_6]DMSO, 50 °C, TMS): $\delta = 0.87$ (t, $J = 6.3$Hz, 9H, CH_3), 1.1–1.9 (overlapped, 84H, $CH_3(CH_2)_{14}$), 3.65 (m, 4H, 3,5-CH_2OAr), 3.79 (t, 2H, 4-CH_2OAr), 6.9 (s, 2H, Ar); ^{13}C NMR ($CDCl_3$/[D_6]DMSO, 50 °C, TMS): $\delta = 14.2$ (CH_3), 22.7 (CH_3CH_2), 25.8 (CH_2CH_2OAr), 28.9–30.3 (CH_2), 31.9 ($CH_3CH_2CH_2$), 69.2 (CH_2OPh), 108.4 (Ar-*C*2,6), 131.5 (Ar-*C*1), 135.2 (Ar-*C*4), 154.1 (Ar-*C*3,5), 176.4 (COO^-); elemental analysis calcd (%) for $C_{55}H_{101}LiO_5$: C 77.78, H 11.99; found: C 77.62, H 11.92.

(3,4,5)16G1-CO_2Na: Starting from **(3,4,5)16G1-CO_2CH_3** and NaOH (0.619 g, 15.5 mmol) in 90% EtOH (100 mL) at 95 °C for 10 h, the title compound was obtained as a white powder (1.84 g, 68.8%) after filtration followed by four recrystallizations from EtOH (90%). Purity (HPLC): 99+%; ^{1}H NMR ($CDCl_3$/[D_6]DMSO, 50 °C, TMS): $\delta = 0.87$ (t, $J = 6.3$ Hz, 9H, CH_3), 1.1–1.9 (overlapped, 84H, $CH_3(CH_2)_{14}$), 3.65 (m, 4H, 3,5-CH_2OAr), 3.79 (t, 2H, 4-CH_2OAr), 6.9 (s, 2H, Ar); ^{13}C NMR ($CDCl_3$/[D_6]DMSO, 50 °C, TMS): $\delta = 14.2$ (CH_3), 22.7 (CH_3CH_2), 25.8 (CH_2CH_2OAr), 28.9–30.3 (CH_2), 31.9 ($CH_3CH_2CH_2$), 69.2 (CH_2OAr), 108.4 (Ar-*C*2,6), 131.5 (Ar-*C*1), 135.2 (Ar-*C*4), 154.1 (Ar-*C*3,5), 176.9 (COO^-); elemental analysis calcd (%) for $C_{55}H_{101}NaO_5 \times 0.5\,H_2O$: C 75.55, H 11.76; found: C 75.44, H 11.76.

(3,4,5)16G1-CO_2K: Starting from **(3,4,5)16G1-CO_2CH_3** and KOH (0.869 g, 15.5 mmol) in 90% EtOH (100 mL) at 95 °C for 10 h, the title compound was obtained as a white powder (1.89 g, 69.5%) after filtration followed by four recrystallizations from EtOH (90%). Purity (HPLC): 99+%; ^{1}H NMR ($CDCl_3$/[D_6]DMSO, 50 °C, TMS): $\delta = 0.87$ (t, $J = 6.3$ Hz, 9H, CH_3), 1.1–1.9 (overlapped, 84H, $CH_3(CH_2)_{14}$), 3.65 (m, 4H, 3,5-CH_2OAr), 3.79 (t, 2H, 4-CH_2OAr), 6.9 (s, 2H, Ar); ^{13}C NMR ($CDCl_3$/[D_6]DMSO, 50 °C, TMS): $\delta = 14.2$ (CH_3), 22.7 (CH_3CH_2), 25.8 (CH_2CH_2OAr), 28.9–30.3 (CH_2), 31.9 ($CH_3CH_2CH_2$), 69.2 (CH_2OAr), 108.4 (Ar-*C*2,6), 131.5 (Ar-*C*1), 135.2 (Ar-*C*4), 154.1 (Ar-*C*3,5), 177.5 (COO^-); elemental analysis calcd (%) for $C_{55}H_{101}KO_5 \times 0.5\,H_2O$: C 74.18, H 11.55; found: C 73.84, H 11.55.

(3,4,5)16G1-CO_2Rb: Starting from **(3,4,5)16G1-CO_2CH_3** (2.65 g, 3.1 mmol) and RbOH 50% wt in H_2O (1.588 g, 15.5 mmol) in 90% EtOH (100 mL) at 95 °C for 10 h, the title compound was obtained as a white powder (2.04 g, 71.2%) after filtration followed by four recrystallizations from EtOH (90%). Purity (HPLC): 99+%; ^{1}H NMR ($CDCl_3$/[D_6]DMSO, 50 °C, TMS): $\delta = 0.87$ (t, $J = 6.3$ Hz, 9H, CH_3), 1.1–1.9 (overlapped, 84H, $CH_3(CH_2)_{14}$), 3.65 (m, 4H, 3,5-CH_2OAr), 3.79 (t, 2H, 4-CH_2OAr), 6.9 (s, 2H, Ar); ^{13}C NMR ($CDCl_3$/[D_6]DMSO, 50 °C, TMS): $\delta = 14.2$ (CH_3), 22.7 (CH_3CH_2), 25.8 (CH_2CH_2OAr), 28.9–30.3 (CH_2), 31.9 ($CH_3CH_2CH_2$), 69.2 (CH_2OAr), 108.4 (Ar-*C*2,6), 131.5 (Ar-*C*1), 135.2 (Ar-*C*4), 154.1 (Ar-*C*3,5), 175.7 (COO^-); elemental analysis calcd (%) for $C_{55}H_{101}O_5Rb$: C 71.20, H 10.97; found: C 71.08, H 10.92.

(3,4,5)18G1-CO_2Li: Starting from **(3,4,5)18G1-CO_2CH_3** (2.91 g, 3.1 mmol) and LiOH (0.372 g, 15.5 mmol) in 90% EtOH (100 mL) at 95 °C for 10 h, the title compound was obtained as a white powder (20.3 g, 70.3%) after filtration followed by four recrystallizations from EtOH (90%). Purity (HPLC): 99+%; ^{1}H NMR ($CDCl_3$/[D_6]DMSO, 50 °C, TMS): $\delta = 0.87$ (t, $J = 6.3$ Hz, CH_3, 9H), 1.1–1.9 (overlapped, 96H, $CH_3(CH_2)_{16}$), 3.65 (m, 4H, 3,5-CH_2OAr), 3.79 (t, 2H, 4-CH_2OAr), 6.9 (s, 2H, Ar); ^{13}C NMR ($CDCl_3$/[D_6]DMSO, 50 °C, TMS): $\delta = 14.2$ (CH_3), 22.7 (CH_3CH_2), 25.8 (CH_2CH_2OAr), 28.9–30.3 (CH_2), 31.9 ($CH_3CH_2CH_2$), 69.2 (CH_2OAr), 108.4 (Ar-*C*2,6), 131.5 (Ar-*C*1), 135.2 (Ar-*C*4), 154.1 (Ar-*C*3,5), 176.4 (COO^-); elemental analysis calcd (%) for $C_{61}H_{113}LiO_5$: C 78.49, H, 12.20; found: C 78.40, H 12.19.

(3,4,5)18G1-CO_2Na: Starting from **(3,4,5)18G1-CO_2CH_3** (2.91 g, 3.1 mmol) and NaOH (0.619 g, 15.5 mmol) in 90% EtOH (100 mL) at 95 °C for 10 h, the title compound was obtained as a white powder (2.04 g, 69.6%) after filtration followed by four recrystallizations from EtOH (90%). Purity (HPLC): 99+%; ^{1}H NMR ($CDCl_3$/[D_6]DMSO, 50 °C, TMS): $\delta = 0.87$ (t, $J = 6.3$ Hz, 9H, CH_3), 1.1–1.9 (overlapped, 96H, $CH_3(CH_2)_{16}$), 3.65 (m, 4H, 3,5-CH_2OAr), 3.79 (t, 2H, 4-CH_2OAr), 6.9 (s, 2H, Ar); ^{13}C NMR ($CDCl_3$/[D_6]DMSO, 50 °C, TMS): $\delta = 14.2$ (CH_3), 22.7 (CH_3CH_2), 25.8 (CH_2CH_2OAr), 28.9–30.3 (CH_2), 31.9 ($CH_3CH_2CH_2$), 69.2 (CH_2OAr), 108.4 (Ar-*C*2,6), 131.5 (Ar-*C*1), 135.2 (Ar-*C*4), 154.1 (Ar-*C*3,5), 176.9 (COO^-); elemental analysis calcd (%) for $C_{61}H_{113}NaO_5$: C 77.16, H 12.00; found: C 77.19, H 11.93.

(3,4,5)18G1-CO_2K: Starting from **(3,4,5)18G1-CO_2CH_3** (2.91 g, 3.1 mmol) and KOH (0.869 g, 15.5 mmol) in 90% EtOH (100 mL) at 95 °C for 10 h, the title compound was obtained as a white powder (2.13 g, 71.4%) after filtration followed by four recrystallizations from EtOH (90%). Purity (HPLC): 99+%; ^{1}H NMR ($CDCl_3$/[D_6]DMSO, 50 °C, TMS): $\delta = 0.87$ (t, $J = 6.3$ Hz, CH_3, 9H), 1.1–1.9 (overlapped, 96H, $CH_3(CH_2)_{16}$), 3.65 (m, 4H, 3,5-CH_2OAr), 3.79 (t, 2H, 4-CH_2OAr), 6.9 (s, 2H, Ar); ^{13}C NMR ($CDCl_3$/[D_6]DMSO, 50 °C, TMS): $\delta = 14.2$ (CH_3), 22.7 (CH_3CH_2), 25.8 (CH_2CH_2OAr), 28.9–30.3 (CH_2), 31.9 (CH_3CH_2 CH_2), 69.2 (CH_2OAr), 108.4 (Ar-*C*2,6), 131.5 (Ar-*C*1), 135.2 (Ar-*C*4), 154.1 (Ar-*C*3,5), 177.3 (COO^-); elemental analysis calcd (%) for $C_{61}H_{113}KO_5$: C 75.87, H 11.79; found: C 75.55, H 11.68.

(3,4,5)18G1-CO_2Rb: Starting from **(3,4,5)18G1-CO_2CH_3** (2.91 g, 3.1 mmol) and RbOH 50% wt in H_2O (1.588 g, 15.5 mmol) in 90% EtOH (100 mL) at 95 °C for 10 h, the title compound was obtained as a white powder (2.26 g, 72.2%) after filtration followed by four recrystallizations from EtOH

  0947-6539/02/0805-1116 $ 17.50+.50/0 *Chem. Eur. J.* **2002**, *8*, No. 5

(90%). Purity (HPLC) 99+%; ^{1}H NMR ($CDCl_3$/[D$_6$]DMSO, 50 °C, TMS): $\delta = 0.87$ (t, $J = 6.3$Hz, 9H, CH_3), 1.1–1.9 (overlapped, 96H, $CH_3(CH_2)_{16}$), 3.65 (m, 4H, 3,5-CH_2OAr), 3.79 (t, 2H, 4-CH_2OAr), 6.9 (s, 2H, Ar); ^{13}C NMR ($CDCl_3$/[D$_6$]DMSO, 50 °C, TMS): $\delta = 14.2$ (CH_3), 22.7 (CH_3CH_2), 25.8 (CH_2CH_2OAr), 28.9–30.3 (CH_2), 31.9 ($CH_3CH_2CH_2$), 69.2 (CH_2OAr), 108.4 (Ar-*C*2,6), 131.5 (Ar-*C*1), 135.2 (Ar-*C*4), 154.1 (Ar-*C*3,5), 175.6 (COO^-); elemental analysis calcd (%) for $C_{61}H_{113}O_5Rb$: C 72.40, H 11.25; found: C 70.04, H 11.36.

(3,4,5)18G1-CO_2Cs: Starting from **(3,4,5)18G1-CO_2CH_3** (2.91 g, 3.1 mmol) and CsOH 50%wt in H_2O (2.32 g, 15.5 mmol) in 90% EtOH (100 mL) at 95 °C for 10 h, the title compound was obtained as a white powder (2.35 g, 71.8%) after filtration followed by four recrystallizations from EtOH (90%). Purity (HPLC): 99+%; ^{1}H NMR ($CDCl_3$/[D$_6$]DMSO, 50 °C, TMS): $\delta = 0.87$ (t, $J = 6.3$ Hz, CH_3, 9H), 1.1–1.9 (overlapped, 96H, $CH_3(CH_2)_{16}$), 3.65 (m, 4H, 3,5-CH_2OAr), 3.79 (t, 2H, 4-CH_2OAr), 6.9 (s, 2H, Ar); ^{13}C NMR ($CDCl_3$/[D$_6$]DMSO, 50 °C, TMS): $\delta = 14.2$ (CH_3), 22.7 (CH_3CH_2), 25.8 (CH_2CH_2OAr), 28.9–30.3 (CH_2), 31.9 ($CH_3CH_2CH_2$), 69.2 (CH_2OAr), 108.4 (Ar-*C*2,6), 131.5 (Ar-*C*1), 135.2 (Ar-*C*4), 154.1 (Ar-*C*3,5), 175.4 (COO^-); elemental analysis calcd (%) for $C_{61}H_{113}CsO_5$: C 69.15, H 10.75; found: C 69.11, H 10.73.

Acknowledgements

Financial support by the National Science Foundation (DMR-99-96288), Office of Naval Research (ONR), Army Research Office (ARO-MURI), the Engineering and Physical Science Research Council (UK), the Synchrotron Radiation Source at Daresbury (UK) and S. Z. D. Cheng of the University of Akron (USA) for the density measurement are gratefully acknowledged.

[1] a) V. S. K. Balagurusamy, G. Ungar, V. Percec, G. Johansson, *J. Am. Chem. Soc.* **1997**, *119*, 1539; b) S. D. Hudson, H.-T. Jung, V. Percec, W.-D. Cho, G. Johansson, G. Ungar, V. S. K. Balagurusamy, *Science* **1997**, *278*, 449; c) V. Percec, W.-D. Cho, P. E. Mosier, G. Ungar, D. J. P. Yeardley, *J. Am. Chem. Soc.* **1998**, *120*, 11061; d) V. Percec, W.-D. Cho, M. Möller, S. A. Prokhorova, G. Ungar, D. J. P. Yeardley, *J. Am. Chem. Soc.* **2000**, *122*, 4249; e) V. Percec, W.-D. Cho, G. Ungar, D. J. P. Yeardley, *Angew. Chem.* **2000**, *112*, 1661; *Angew. Chem. Int. Ed.* **2000**, *39*, 1597; f) V. Percec, W.-D. Cho, G. Ungar, *J. Am. Chem. Soc.* **2000**, *122*, 10273; g) V. Percec, W.-D. Cho, G. Ungar, D. J. P. Yeardley, *J. Am. Chem. Soc.* **2001**, *123*, 1302.

[2] a) D. J. P. Yeardley, G. Ungar, V. Percec, M. N. Holerca, G. Johansson, *J. Am. Chem. Soc.* **2000**, *122*, 1684; b) H. Duan, S. D. Hudson, G. Ungar, M. N. Holerca, V. Percec, *Chem. Eur. J.* **2001**, *7*, 4134.

[3] a) V. Percec, G. Johansson, J. Heck, G. Ungar, S. V. Batty, *J. Chem. Soc. Perkin Trans. 1* **1993**, 1411; b) G. Johansson, V. Percec, G. Ungar, D. Abramic, *J. Chem. Soc. Perkin Trans. 1* **1994**, 447; c) V. Percec, G. Johansson, G. Ungar, J. Zhou, *J. Am. Chem. Soc.* **1996**, *118*, 9855.

[4] a) D. J. Pesak, J. S. Moore, *Angew. Chem.* **1997**, *109*, 1709; *Angew. Chem. Int. Ed. Engl.* **1997**, *36*, 1636; b) M. Suárez, J.-M. Lehn, S. C. Zimmerman, A. Skoulios, B. Heinrich, *J. Am. Chem. Soc.* **1998**, *120*, 9526; c) H. Meier, M. Lehmann, *Angew. Chem.* **1998**, *110*, 666; *Angew. Chem. Int. Ed. Engl.* **1998**, *37*, 643.

[5] a) V. Percec, C.-H. Ahn, G. Ungar, D. J. P. Yeardley, M. Möller, S. S. Sheiko, *Nature* **1998**, *391*, 161; b) V. Percec, C.-H. Ahn, W.-D. Cho, A. M. Jamieson, J. Kim, T. Leman, M. Schmidt, M. Gerle, M. Möller, S. A. Prokhorova, S. S. Sheiko, S. Z. D. Cheng, A. Zhang, G. Ungar, D. J. P. Yeardley, *J. Am. Chem. Soc.* **1998**, *120*, 8619; c) J. O. Jeppesen, J. Perkins, J. Becher, J. F. Stoddart, *Angew. Chem.* **2001**, *113*, 1256; *Angew. Chem. Int. Ed.* **2001**, *40*, 1216; d) H. Tamiaki, T. Obata, Y. Azefu, K. Toma, *Bull. Chem. Soc. Jpn.* **2001**, *74*, 733; e) Z. Bao, K. R. Amundson, A. J. Lovinger, *Macromolecules* **1998**, *31*, 8647; f) R. Jakubiak, Z. Bao, L. J. Rothberg, *Synth. Met.* **2000**, *114*, 61; g) R. Jakubiak, Z. Bao, L. J. Rothberg, *Synth. Met.* **2001**, *116*, 41.

[6] a) V. Percec, P. Chu, G. Ungar, J. Zhou, *J. Am. Chem. Soc.* **1995**, *117*, 11441; b) V. Percec, C.-H. Ahn, B. Barboiu, *J. Am. Chem. Soc.* **1997**, *119*, 12978; c) V. Percec, M. N. Holerca, *Biomacromolecules* **2000**, *1*, 6; d) V. Percec, M. N. Holerca, S. N. Magonov, D. J. P. Yeardley, G. Ungar, H. Duan, S. D. Hudson, *Biomacromolecules* **2001**, *2*, 706; e) V. Percec, M. N. Holerca, S. Uchida, D. J. P. Yeardley, G. Ungar, *Biomacromolecules* **2001**, *2*, 729.

[7] V. Percec, C.-H. Ahn, T. K. Bera, G. Ungar, D. J. P. Yeardley, *Chem. Eur. J.* **1999**, *5*, 1070.

[8] D. E. Robertson, R. S. Farid, C. C. Moser, J. L. Urbauer, S. E. Mulholland, R. Pidikiti, J. D. Lear, A. J. Wand, W. F. DeGrado, P. L. Dutton, *Nature* **1994**, *368*, 425.

[9] a) G. Ungar, D. Abramic, V. Percec, J. A. Heck, *Liq. Cryst.* **1996**, *21*, 73; b) G. Ungar, V. Percec, M. N. Holerca, G. Johansson, J. Heck, *Chem. Eur. J.* **2000**, *6*, 1258.

[10] For several representative publications on liquid crystals from metal salts, see: a) D. Vorländer, *Ber. Dtsch. Chem. Ges.* **1910**, *43*, 3120; b) A. Skoulios, V. Luzzati, *Nature* **1959**, *183*, 1310; c) A. R. Ubbelohde, *Nature* **1973**, *244*, 487; d) M. J. Baena, P. Espinet, M. C. Lequerica, A. M. Levelut, *J. Am. Chem. Soc.* **1992**, *114*, 4182; e) B. Heinrich, K. Praefcke, D. Guillon, *J. Mater. Chem.* **1997**, *7*, 1363.

[11] For some reviews on liquid crystals from metal salts, see: a) T. A. Mirnaya, V. D. Prisyazhnyi, V. A. Shcherbakov, *Russ. Chem. Rev.* **1989**, *58*, 821; b) A.-M. Giroud-Godquin, P. M. Maitlis, *Angew. Chem.* **1991**, *103*, 370; *Angew. Chem. Int. Ed. Engl.* **1991**, *30*, 375; c) A. P. Polishchuk, T. V. Timofeeva, *Russ. Chem. Rev.* **1993**, *62*, 291; d) P. Espinet, M. A. Esteruelas, L. A. Oro, J. L. Serrano, E. Sola, *Coord. Chem. Rev.* **1992**, *117*, 215; e) S. A. Hudson, P. M. Maitlis, *Chem. Rev.* **1993**, *93*, 861.

[12] For several reviews and books on metal complexes containing mesogens, see: a) L. Oriol, J. L Serrano, *Adv. Mater.* **1995**, *7*, 348; b) D. W. Bruce, *Acc. Chem. Res.* **2000**, *33*, 831; c) J.-C. P. Gabriel, P. Davidson, *Adv. Mater.* **2000**, *12*, 9; d) *Metallomesogens* (Ed.: J. L. Serrano), Wiley-VCH, Weinheim, **1995**.

[13] a) J. Heck, Ph.D. Thesis, Case Western Reserve University, Cleveland, OH, **1995**; b) M. N. Holerca, Ph.D. Thesis, University of Pennsylvania, Philadelphia, PA, **2001**.

[14] P. Ziherl, R. D. Kamien, *Phys. Rev. Lett.* **2000**, *85*, 3528.

[15] a) D. A. Tomalia. *Adv. Mater.* **1994**, *6*, 529; b) J. M. J. Fréchet, *Science* **1994**, *263*, 1710; c) G. R. Newkome, C. N. Moorefield, F. Vögtle, *Dendritic Molecules. Concepts*, *Synthesis*, *Perspectives*, VCH, Weinheim, **1996**; d) J. S. Moore, *Acc. Chem. Res.* **1997**, *30*, 402; e) F. Zeng, S. C. Zimmerman, *Chem. Rev.* **1997**, *97*, 1681; f) D. K. Smith, F. Diederich, *Chem. Eur. J.* **1998**, *4*, 1353; g) H. Frey, *Angew. Chem.* **1998**, *110*, 2113; *Angew. Chem. Int. Ed.* **1998**, *37*, 2193; h) O. A. Mathews, A. N. Shipway, J. F. Stoddart, *Prog. Polym. Sci.* **1998**, *23*, 1; i) A. W. Bosman, H. M. Janssen, E. W. Meijer, *Chem. Rev.* **1999**, *99*, 1665; j) A. J. Berresheim, M. Müller, K. Müllen, *Chem. Rev.* **1999**, *99*, 1747; k) D. K. Smith, F. Diederich, *Top. Curr. Chem.* **2000**, *210*, 183.

[16] a) R. C. Smith, W. M. Fischer, D. L. Gin, *J. Am. Chem. Soc.* **1997**, *119*, 4092; b) H. Deng, D. L. Gin, R. C. Smith, *J. Am. Chem. Soc.* **1998**, *120*, 3522; c) J. H. Ding, D. L. Gin, *Chem. Mater.* **2000**, *12*, 22; d) R. Resel, G. Leising, P. Markart, M. Kriechbaum, R. Smith, D. L. Gin, *Macromol. Chem. Phys.* **2000**, *201*, 1128.

[17] a) M. Kawa, J. M. J. Fréchet, *J. Chem. Mater.* **1998**, *10*, 286; b) M. Kawa, J. M. J. Fréchet, *Thin Solid Films* **1998**, *331*, 259.

[18] a) J. L. M. van Nunen, B. F. B. Folmer, R. J. M. Nolte, *J. Am. Chem. Soc.* **1997**, *119*, 283; b) B. Xu, T. M. Swager, *J. Am. Chem. Soc.* **1993**, *115*, 1159; c) C. Tschierske, *J. Mater. Chem.* **1998**, *8*, 1485; d) K. Borisch, S. Diele, P. Göring, H. Kresse, C. Tschierske, *J. Mater. Chem.* **1998**, *8*, 529.

Received: August 3, 2001 [F3469]